American Mineralogist, Volume 73, pages 1302–1324, 1988

Fluid infiltration through the Big Horse Limestone Member in the Notch Peak contact-metamorphic aureole, Utah

Theodore C. Labotka
Department of Geological Sciences, University of Tennessee, Knoxville, Tennessee 37996, U.S.A.
Peter I. Nabelek
Department of Geology, University of Missouri, Columbia, Missouri 65211, U.S.A.
J. J. Papike
Institute for the Study of Mineral Deposits, South Dakota School of Mines and Technology, Rapid City, South Dakota 57701, U.S.A.

Abstract

Calcareous argillites in the Upper Cambrian Big Horse Limestone Member of the Orr Formation, west-central Utah, have undergone contact metamorphism where they were intruded by the Jurassic Notch Peak stock. Metamorphism of the rocks resulted in nearly complete decarbonation, yet the mineral assemblages indicate that the fluid phase was nearly free of CO_2, indicating interaction with a substantial volume of water. This study is designed to determine the volume of externally derived water with which the Big Horse Limestone Member interacted and the mode of interaction. The rocks in the aureole are characterized by three grades of metamorphism, separated by the diopside and the wollastonite isograds. Assemblages in incipiently metamorphosed samples are calcite + quartz + muscovite + biotite + chlorite + plagioclase. Diopside-zone samples contain calcite + quartz + diopside + tremolite + phlogopite + K-feldspar + plagioclase or a subset of this assemblage. Wollastonite-zone assemblages are typified by calcite + wollastonite + diopside + vesuvianite + grossular + K-feldspar + plagioclase. Conditions within the diopside zone, determined from calcite + dolomite temperatures of interbedded dolomitic marbles and from the phase equilibria in the system CaO-MgO-Al_2O_3-SiO_2-$KAlSi_3O_8$-CO_2-H_2O, were about 434 °C and $x_{CO_2} = 0.024$, at a pressure of 2 kbar. These are the inferred conditions for the invariant assemblage calcite + quartz + tremolite + diopside + phlogopite + K-feldspar, which occurs locally in the diopside zone. Conditions in the wollastonite zone appear to have been $T > 450$ °C, $x_{CO_2} \leq 0.002$. The amounts of volatiles released by the rocks were calculated by the mass balance protolith → metamorphic rock, balanced by appropriate amounts of H_2O and CO_2. Diopside-zone rocks evolved 45 ± 23 g of CO_2 and 16 ± 7 g of H_2O per kilogram of protolith. Wollastonite-zone rocks released 158 ± 45 g of CO_2 and 10 ± 3 g of H_2O per kilogram of protolith. The amounts of H_2O required to maintain the equilibrium fluid compositions are 0.73 ± 0.36 kg of H_2O per kilogram of rock in the diopside zone and 11.2 ± 5.0 kg of H_2O per kilogram of rock in the wollastonite zone. This water/rock ratio in the wollastonite zone is about 25 times that indicated by stable-isotope studies on the same rocks. The T-x_{CO_2} path of metamorphism of this rock was (1) at the diopside isograd, the conditions were near, but below, the invariant point calcite + quartz + tremolite + diopside + phlogopite + K-feldspar; (2) minor reaction buffered the conditions to those of the invariant point, 434 °C, $x_{CO_2} = 0.024$, which represents the megascopically recognizable diopside isograd; (3) infiltration of 0.3 rock masses of H_2O drove the reaction phlogopite + 3 calcite + 6 quartz = 3 diopside + K-feldspar + $3CO_2$ + H_2O to completion; (4) the reaction tremolite + 3 calcite + 2 quartz + 5 diopside + $3CO_2$ + H_2O occurred throughout the diopside zone until tremolite was consumed, when $T = 464$ °C and $x_{CO_2} = 0.04$; and (5) infiltration of at least 13.3 rock masses of H_2O at the wollastonite isograd was required to drive the reaction calcite + quartz = wollastonite + CO_2 to completion at $T = 464$ °C, $x_{CO_2} = 0.004$. Infiltration was abetted by the reduction in solid volume of 25%. The high water/rock ratio in the wollastonite zone combined with the low water/rock ratio in the diopside zone indicates that the high ratio does not represent the fluid flux, but rather the volume of the fluid reservoir with which the wollastonite-zone rocks equilibrated. Mass-balance calculations show that there was more than sufficient H_2O in the pore space in the Notch Peak

0003–004X/88/1112–1302$02.00

stock to have acted as the reservoir. The reaction front represented by the wollastonite isograd was the final outermost locus of effective mixing between the reservoir and the evolved fluid, and the position of the front was governed by the rates of diffusion of CO_2 through the fluid and of heat transfer through the rock. Simple calculations of the temperature and fluid flux through the aureole, based on heat- and fluid-transport equations, indicate that heat transport on the margins of the stock occurred primarily by conduction, particularly outside the wollastonite zone, and that the major fluid flux through the aureole occurred within the first year of intrusion, long before the temperature had risen sufficiently for metamorphism to have occurred. Fluid fluxes through the aureole after 1000 yr, when significant metamorphism occurred, dropped to the order of 1 kg/(m^2·yr), or less. This amount is sufficient to have interacted with the diopside-zone rocks, giving water/rock ratios (by mass) of the order 0.1. The fluid flux through the wollastonite zone is given by the rate of advancement of the isograd, which gives fluxes ranging from >42 kg/(m^2·yr) at 50 m from the contact to 0 kg/(m^2·yr) at the maximum distance of 410 m. The results of this study indicate that in those metamorphic terranes in which there is a change from rock-dominated to fluid-dominated systems across an isograd, the water/rock ratio in the fluid-dominated system represents not the fluid flux, but the mass of fluid in a reservoir with which the rocks equilibrated.

Introduction

The fluid phase in metamorphic terranes is the major agent for the transport of mass and, in some cases, heat through the crust. Knowledge of the composition and flux of the fluid phase is vital to the determination of chemical differentiation processes occurring in the middle and upper parts of the crust. Yet, like the fugitive components that make up the fluid, the fluid phase has fled the ancient geothermal systems, now exposed at Earth's surface as metamorphic terranes. Minerals in the metamorphic rocks and their fluid inclusions, if any, are the only remaining evidence of the fluid. The nature of the fluid—its composition, flux, source, and destination—must be inferred from the compositions and abundances of the minerals in the rock or, in some cases, from the fluid inclusions.

It is clear from simple calculations (Walther and Orville, 1982) that fluids within the crust must migrate, and this migration can result in the dissipation of heat and dissolved ions through the crust. Because most metamorphic rocks have porosities much less than 1%, fluids generated by metamorphic reactions must have escaped into a hydrothermal system consisting of a mixture of evolved and infiltrating fluids. By means of mineral reactions, the rock maintains equilibrium with the fluid during changes in intensive variables. Thus, the compositions and abundances of the minerals monitor the fluid's composition and abundance. There can be a complex interplay between the compositions and volumes of evolved and infiltrating fluids. At one extreme, equilibrium fluid compositions can reflect the stoichiometric ratios of the volatile components evolved by the rock if there is little or no infiltration. At the other extreme, during infiltration of substantial amounts of externally derived fluid, the buffer capacity of the rock can be exceeded, and the equilibrium fluid composition will reflect the composition of the infiltrating fluid. Reality lies between the extremes, particularly in contact-metamorphic aureoles, in which a convecting, infiltrating fluid phase recycles through the metamorphic terrane, mixes with fluids evolved from the metamorphic rock, escapes to the surface, and is recharged with fluid added to the geothermal system.

Previous studies of metamorphosed carbonate rocks in contact and regional metamorphic terranes have documented both rock-dominated (e.g., Rice, 1977; Hover-Granath et al., 1983; Labotka, 1981) and fluid-dominated (e.g., Ferry, 1987; Bucher-Nurminen, 1981; Rumble et al., 1982; Hover-Granath et al., 1983; Bebout and Carlson, 1986) behavior. The behavior of fluids in contact-metamorphic environments depends on the rock types and the geometry of the aureole. Nowhere is this more clearly evident than in the aureole of the Notch Peak stock. The work of Hover-Granath et al. (1983) and Nabelek et al. (1984) has shown that relatively pure carbonate rocks were impervious to fluids, whereas interbedded argillaceous carbonate rocks acted as aquifers for fluids emigrating from the stock.

The purpose of this paper is to determine the nature of the physical process of infiltration in the contact-metamorphic aureole of the Notch Peak stock and to establish the meaning of the water/rock ratio in the permeable calcareous argillites. The procedure used to determine amount of fluid that interacted with the argillites is to calculate the mass balance between metamorphic rocks and their unmetamorphosed protoliths. A companion paper, Labotka et al. (1988), examines the systematics of the bulk rock chemistry to establish the validity of the mass-balance calculations presented here. The method is described by Labotka et al. (1984) and is similar to the reaction-progress method of Ferry (1983). The result is the amount and composition of the fluid evolved by the rock during metamorphism. The amount of externally derived fluid is determined by comparison of the evolved fluid with the equilibrium X_{CO_2} value determined from the mineral assemblages. The water/rock ratios calculat-

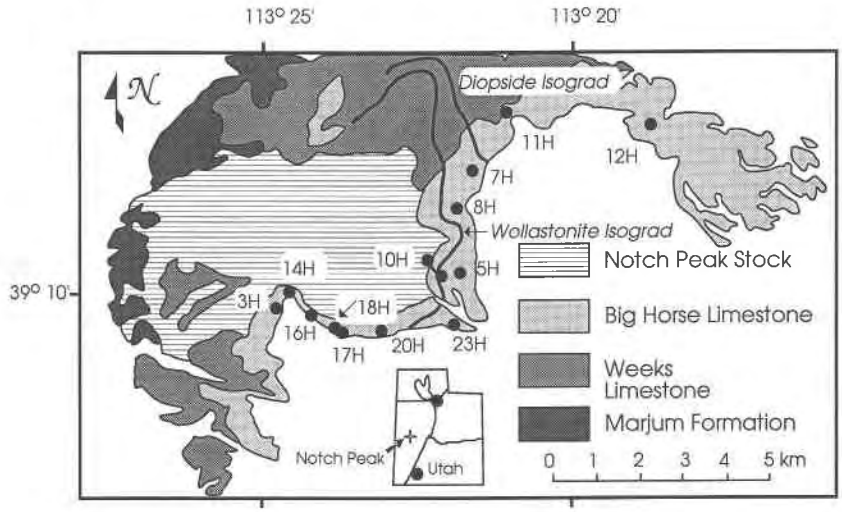

Fig. 1. Generalized geologic map of a portion of the Notch Peak quadrangle, Utah, modified from Hintze (1974), showing sample localities and the diopside and wollastonite isograds based on assemblages in calcareous argillites in the Big Horse Limestone Member of the Orr Formation and in the Weeks Limestone.

ed by this method vary considerably over the metamorphic aureole, and this variation is examined for the relation between the ratio and the amount of fluid that infiltrated the aureole. Rate of infiltration, that is, the fluid flux, is estimated from a simple model for heat and mass transport in the aureole. The integrated flux from this model is then compared with the water/rock ratios calculated from the mass balance. The results indicate that fluid fluxes are consistent with water/rock ratios for rock-dominated, or buffered, systems. Water/rock ratios in fluid-dominated systems can overestimate the flux by several orders of magnitude. In these cases, the water/rock ratio indicates the amount of fluid that interacted with the rock; however, this fluid did not infiltrate the rock, but occupied a reservoir that effectively communicated with the rock.

Geology and petrology of the Notch Peak aureole

The Notch Peak stock, located in west-central Utah, intruded the Upper Cambrian Weeks Formation and the Big Horse Limestone Member of the Orr Formation during Jurassic time (Fig. 1). The Notch Peak stock is an ovoid composite of granite and quartz monzonite intrusions; the petrogenesis of the granitic rocks is described by Nabelek et al. (1986). The stock discordantly intrudes the gently dipping Big Horse Limestone Member, which can be traced along strike for more than 6 km. The stratigraphy of the Big Horse Limestone Member consists of six upward-shallowing cycles, each comprising thinly interbedded calcareous mudstones and quartz-rich siltstones, capped by algal or oolitic limestone. The individual cycles can be traced directly to the contact with the Notch Peak stock.

The petrology of the contact-metamorphosed Big Horse Limestone Member was described by Hover-Granath et al. (1983). At low grades, the limestone marbles contain assemblages characterized by calcite + dolomite + talc and calcite + talc + tremolite. At medium grade, talc is replaced by diopside in the assemblage. The highest-grade marbles contain forsterite. Although the marbles consist predominantly of calcite and dolomite, most samples contain low-variance assemblages; divariant assemblages in the system CaO-MgO-SiO_2-H_2O-CO_2 are common, and univariant assemblages occur. These assemblages indicate that the equilibrium values of P_{CO_2} and P_{H_2O} were buffered by the mineral reactions. In addition, the domains of equilibrium were found to be smaller than the area sampled by a thin section, indicating local control of μ_{CO_2} and μ_{H_2O} by the rock. At a pressure of 2 kbar, an estimate based on the amount of stratigraphic overburden during Jurassic time, the mineral assemblages appear to have buffered x_{CO_2} to values as high as 0.8 at temperatures as high as 575 °C.

The calcareous argillites contain radically different assemblages from those in the marbles, reflecting the differences in rock composition and in fluid composition during metamorphism of the two rock types. Unmetamorphosed or very low grade argillites contain calcite + quartz + albite + chlorite, phlogopite, muscovite, or K-feldspar. Low-grade rocks contain the assemblage calcite + quartz + diopside + K-feldspar + calcic plagioclase. Many samples contain tremolite in addition. At high metamorphic grade, the argillites are characterized by the assemblage calcite + wollastonite + diopside + grossular + vesuvianite + K-feldspar + albite. These assemblages are stable in very H_2O-rich fluids. Two isograds are shown in Figure 1, based on these assemblages. The lower-grade isograd is the first appearance of diopside. Rocks at lower grade than the diopside isograd are only incipiently metamorphosed or are unmetamorphosed. The higher-grade isograd marks the first appear-

Table 1. Samples of the Big Horse Limestone Member of the Orr Formation

Sample	Map distance from contact (m)	Metamorphic grade*	Mineral assemblage**	Temperature† (°C)	Fluid composition‡ (x_{CO_2})
			Cycle 1 argillites		
14H-80	72 ± 48§	High	Cal + Wo + Diop + Ves + Gross + Ksp + Plag	466 ± 156	0.0014(0.0054)
16H-84	120	High	Cal + Wo + Diop + Ves + Gross + Ksp + Plag	519 ± 18	0.0642(0.0183)
3H-37	240	High	Cal + Wo + Diop + Ves + Gross + Ksp + Plag	495 ± 34	0.0015(0.0108)
3H-36	240	High	Cal + Wo + Diop + Gross + Ksp + Plag	495 ± 34	0.0500(0.0108)
18H-89	240	High	Cal + Wo + Diop + Ves + Gross + Ksp	481 ± 17	0.0056(0.0075)
20H-98	360	High	Cal + Wo + Diop + Gross + Ksp + Plag	445 ± 29	(0.0031)
5H-47	720	Low	Cal + Qtz + Trem + Diop + Scap + Ksp	447 ± 21	0.0299
23H-137	720	Low	Cal + Qtz + Bio + Trem + Ksp + Plag		—
8H-129	960	Low	Cal + Qtz + Diop + Gross + Scap + Ksp + Plag		—
7H-56	1440	Low	Cal + Qtz + Trem + Diop + Ksp + Plag	428 ± 14	0.0176
11H-115	2400	Unmet.	Cal + Qtz + Musc + Bio + Plag	248 ± 2	
			Cycle 2 argillites		
16H-86	120	High	Cal + Wo + Diop + Ves + Gross + Ksp + Plag	519 ± 18	0.0032(0.0183)
3H-40	204	High	Cal + Wo + Diop + Ves	495 ± 34	(0.0108)
3H-39	240	High	Cal + Wo + Diop + Ves + Ksp + Plag	495 ± 34	(0.0108)
17H-87	240	High	Cal + Wo + Diop + Ves + Gross + Ksp + Plag		—
20H-100	360	High	Cal + Wo + Diop + Ves + Plag	445 ± 29	(0.0031)
5H-44	720	Low	Cal + Qtz + Bio + Diop + Ksp + Plag	447 ± 21	0.0388
23H-135	720	Low	Cal + Qtz + Bio + Trem + Diop + Ksp + Plag		—
8H-59	960	Low	Cal + Bio + Diop + Ves + Ksp + Plag		—
7H-54A	1440	Low	Cal + Qtz + Bio + Trem + Diop + Scap + Ksp + Plag	428 ± 14	0.0176, 0.0193
11H-117	2400	Unmet.	Cal + Qtz + Musc + Ksp + Plag	248 ± 23	
12H-123	5280	Unmet.	Cal + Qtz + Musc + Bio + Ksp + Plag	274 ± 76	

* Grade represented by mineral assemblages in argillites. High ≡ wollastonite zone. Low ≡ diopside zone. Unmet. ≡ unmetamorphosed or incipiently metamorphosed.

** Complete mineral assemblages, including minor and trace minerals, are given in Hover-Granath et al. (1983).

† Temperatures are from calcite + dolomite equilibria in adjacent limestones. Errors represent homogeneity of calcite. From Hover-Granath et al. (1983).

‡ Calculated from the equilibria listed in Table 4 at the given temperature and 2000 bars. Multiple values represent separate equilibria. Values in parentheses are upper limits imposed by wollastonite stability.

§ Error represents uncertainty in sample location.

ance of wollastonite. Isograds based on reactions in the marbles are described by Hover-Granath et al. (1983).

Samples

Twenty-two argillite samples from the top two cycles of the Big Horse Limestone Member were analyzed for major and trace elements by X-ray fluorescence and instrumental neutron-activation analysis. The methods of analysis are described in Labotka et al. (1988). O-, C-, and H-isotope analyses were determined on these samples by Nabelek et al. (1984). Microprobe analyses of the minerals in these samples were obtained by Hover (1981). These data are integrated here to determine the balance between the amount and composition of fluid evolved from the argillite and the amount and composition derived external to the rock. The sample locations are shown in Figure 1. Table 1 lists the samples and their mineral assemblages. The samples are divided into three groups according to their mineral assemblages. Wollastonite-zone rocks (high grade) contain calcite + wollastonite + grossular + vesuvianite + diopside, diopside-zone rocks (low grade) contain calcite + quartz + diopside and generally lack grossular and vesuvianite, and unmetamorphosed rocks lack tremolite or diopside although some have almost certainly undergone phlogopite-forming reactions.

The approximate distances of the samples from the contact with the stock are also given in Table 1. The wollastonite isograd, which separates the diopside zone from the wollastonite zone occurs at a distance of about 500 ± 150 m from the contact. The isograd is closer to the contact on the south and southeast side of the stock than it is on the east and northeast side. The difference may be related to the geometry of the stock; the southeast wall is nearly vertical, whereas the northeast contact dips gently outward.

The temperature of metamorphism of the samples, shown in Table 1, is taken from the calcite-dolomite temperature recorded by the cycle 2 limestone between the argillite samples and is from Hover-Granath et al. (1983). Most argillite samples lack mineral assemblages appropriate for calculating the metamorphic temperature, so the temperatures of the adjacent limestones were used in phase-equilibrium calculations and as constraints on the calculated temperature from heat flow. Hover-Granath et al. (1983) showed that these temperatures were consistent with the mineral assemblages in the limestone samples.

The major-element bulk compositions of the argillites are given in Table 2 of Labotka et al. (1988). Changes in the bulk composition with metamorphic grade are discussed by Labotka et al. (1988) who found no systematic change in the composition with metamorphic grade, except for the loss of CO_2. There is some evidence for nonsystematic redistribution of feldspar components, particularly Sr, in some high-grade samples. However, there

TABLE 2. Representative mineral analyses from argillites of the Big Horse Limestone Member

Mineral:	Chlorite	Muscovite	Biotite	Biotite	Tremolite	Diopside	Diopside	Grossular	Vesuvianite	K-feldspar	Plagioclase	Plagioclase	Plagioclase
Grade:	Low	Unmet.	Unmet.	Low	Low	Low	High	High	High	High	Unmet.	Low	High
Sample:	5H-44	12H-123	11H-115	5H-44	5H-47	5H-44	14H-80	14H-80	14H-80	14H-80	11H-115	5H-44	14H-80
Reference:	5-16A	1-33	1-9	1-54	3-53	3-27	3-4	2-22	1-4	1-21	1-5	4-23	1-22
SiO_2	30.28	45.59	40.79	41.57	55.48	53.18	52.27	37.66	35.97	65.59	67.88	44.47	69.90
TiO_2	0.00	0.80	0.41	0.19	0.01	0.24	0.02	1.13	3.57	—	—	—	—
Al_2O_3	19.25	30.59	17.34	12.29	2.57	1.54	0.70	11.75	15.14	18.46	20.03	35.36	19.47
Cr_2O_3	0.10	0.03	0.02	0.00	0.00	0.00	0.01	0.00	0.00	—	—	—	—
FeO	13.27	5.40	5.80	8.44	5.71	5.87	11.15	12.17	4.60	0.00	0.05	0.08	0.09
MnO	0.20	0.03	0.02	0.08	0.00	0.10	0.17	0.18	0.04	—	—	—	—
MgO	23.23	1.39	20.56	22.04	21.03	14.38	11.15	0.00	1.13	—	—	—	—
CaO	0.19	0.66	0.49	0.10	13.03	24.41	23.36	35.11	34.97	0.12	0.67	18.35	0.29
Na_2O	0.00	0.19	0.06	0.00	0.28	0.11	0.14	—	0.29	0.51	11.38	1.07	11.65
K_2O	0.26	10.06	9.34	10.69	0.32	—	—	—	—	15.98	0.12	0.47	0.05
Total	86.78	94.74	94.83	95.40	98.43	99.83	99.97	98.00	95.71	100.66	100.13	99.80	101.45
						Cation proportions							
Si	3.01	3.13	2.90	3.01	7.66	1.97	2.00	3.00	17.97	3.00	2.97	2.06	3.01
Ti	0.00	0.04	0.02	0.01	0.00	0.01	0.00	0.07	1.34				
Al	2.25	2.47	1.45	1.05	0.42	0.06	0.03	1.10	8.92	1.00	1.03	1.93	0.99
Cr	0.01	0.00	0.00	0.00	0.00	0.00	0.00	0.00	0.00				
Fe^{3+}*					0.12	0.00	0.00	0.81	1.92				
Fe	1.10	0.31	0.34	0.51	0.54	0.18	0.36	0.00	0.00	0.00	0.00	0.00	0.00
Mn	0.02	0.00	0.00	0.00	0.00	0.00	0.01	0.01	0.02				
Mg	3.44	0.14	2.18	2.38	4.33	0.79	0.64	0.00	0.84				
Ca	0.02	0.05	0.04	0.01	1.93	0.97	0.96	2.99	18.72	0.01	0.03	0.91	0.01
Na	0	0.02	0.01	0	0.08	0.01	0.01		0.28	0.04	0.96	0.10	0.97
K	0.03	0.88	0.85	0.99	0.06					0.93	0.01	0.03	0.00

* Calculated via the method of Papike et al. (1974).

appears to have been no change in the ratios of major elements during metamorphism. The mass balance between unmetamorphosed and high-grade samples can then be calculated by preserving major-element ratios.

The representative compositions of minerals from unmetamorphosed, diopside-zone, and wollastonite-zone samples are given in Table 2. A complete set of analyses have been deposited.[1] These were determined by microprobe analysis using an automated ARL EMX microprobe at the State University of New York at Stony Brook. Analytical conditions are completely described by Hover (1981). These mineral compositions are used in the mass-balance calculations in which the major cations are distributed among the coexisting minerals.

FLUID COMPOSITION

The first step in determining the amount of fluid infiltration that occurred during metamorphism of the argillites is to determine the composition of the fluid in equilibrium with the mineral assemblages. Hover-Granath et al. (1983) outlined the general composition of the fluid in equilibrium with argillites using T-x_{CO_2} diagrams showing the reaction paths based on the textures of the rocks. Here the equilibria and compositions are calculated to establish the range in conditions that prevailed within the diopside and wollastonite zones. In this section, the fluid compositions are estimated quantitatively from the thermodynamic data of Helgeson et al. (1978), as tabulated by Rice (1983), and the H_2O-CO_2 mixing properties given by Kerrick and Jacobs (1981). The Kerrick and Jacobs fugacities give x_{CO_2} that is about 9% more H_2O rich than those of Holloway (1977) for H_2O-rich fluids. This error is small compared with the uncertainties in the data themselves, as discussed below.

Diopside zone

The diopside isograd represents the change from phlogopite + calcite + quartz assemblages in unmetamorphosed rocks to diopside + K-feldspar assemblages. Many diopside-zone rocks contain all these minerals plus tremolite. The six-phase assemblage is invariant in the system SiO_2-$KAlSi_3O_8$-MgO-CaO-CO_2-H_2O at a constant pressure and with a binary CO_2-H_2O fluid. Rice (1977) described two reactions within this system, 5 phlogopite + 6 calcite + 24 quartz = 3 tremolite + 5 K-feldspar + $6CO_2$ + $2H_2O$ and 3 tremolite + 6 calcite + K-feldspar = 12 diopside + phlogopite + $6CO_2$ + $2H_2O$. A third reaction, which is a linear combination of these two, is phlogopite + 3 calcite + 6 quartz = K-feldspar + 3 diopside + $3CO_2$ + H_2O. This reaction best represents the diopside isograd in the aureole of the Notch Peak stock because the products represent the diopside-zone assemblage, whereas the reactants occur in the unmetamorphosed rocks. The intersection of the two reactions described by Rice (1977) occurs at the T-x_{CO_2} conditions 360 °C and 0.002, based on the fugacity coefficients of

[1] A copy of the analyses may be ordered as Document AM-88-393 from the Business Office, Mineralogical Society of America, 1625 I Street, N.W., Suite 414, Washington, D.C. 20006, U.S.A. Please remit $5.00 in advance for the microfiche.

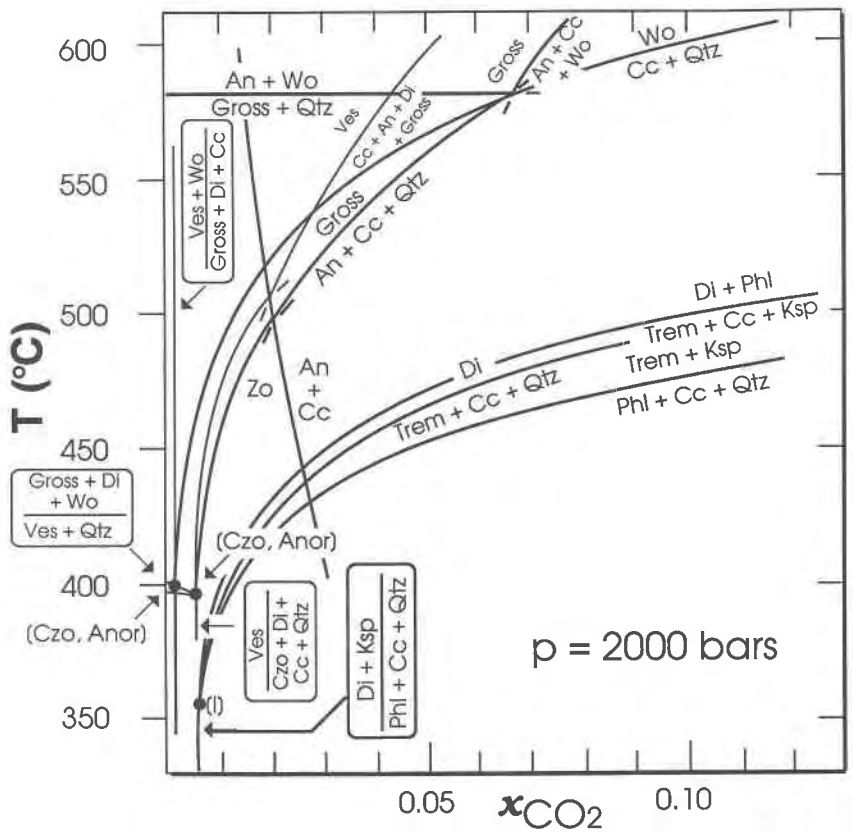

Fig. 2. The H_2O-rich portion of the 2-kbar T-x_{CO_2} diagram showing reactions that affected the Big Horse Limestone Member. Heavy lines were calculated from available thermodynamic data, and light lines are reactions involving vesuvianite with positions constrained by experimental data. The details around the invariant points [Wo, An] and [An, Czo] can be seen in Hover-Granath et al. (1983). Invariant point [I] represents the assemblage calcite + quartz + phlogopite + K-feldspar + diopside + tremolite.

Kerrick and Jacobs (1981). The calculated equilibria are shown in Figure 2, and the stoichiometry of the reactions and their equilibrium constants are given in Table 3; the equilibrium-constant expressions were taken from compilations of Rice (1977, 1983). In the vicinity of the invariant point, all the reactions nearly coincide and have steep, nearly vertical slopes. For example, on the low-temperature side of the invariant point, the reactions 3 calcite + tremolite + 2 quartz = 5 diopside + $3CO_2$ + H_2O and 3 calcite + phlogopite + 6 quartz = 3 diopside + K-feldspar + $3CO_2$ + H_2O are separated by only 0.00001 in x_{CO_2} at 330 °C—an amount strictly unresolvable within the errors in the thermodynamic quantities—and x_{CO_2} increases by a value of 0.0004 over the temperature increase from 330 to 360 °C.

Calcite-dolomite temperatures recorded by the diopside-zone rocks range from 428 ± 14 °C to 447 ± 21 °C, indicating that the temperature of 360 °C for the invariant point is probably too low. The fluid compositions calculated from the recorded temperatures and the equilibria in Table 3 are listed in Table 1 and range from x_{CO_2} = 0.018 to 0.034. The midpoint of the overlapping errors in temperature is 434 °C, and the average value of x_{CO_2} is 0.024; these values are taken to be those of the invariant point. No attempt is made here to correct the values used to calculate Figure 2.

The assemblage within the diopside zone is strictly univariant because of Fe substitution for Mg. The diopside in sample 5H-44 (Table 2) has a value of Mg/(Mg + Fe) = 0.81, and the biotite has a value of 0.82. In sample 23H-135, the Mg/(Mg + Fe) value of diopside ranges from 0.61 to 0.67, the tremolite has a value of 0.64 to 0.65, and the biotite has a value of 0.64. The partitioning of Fe and Mg among the phases is almost equal, and, therefore, the substitution of Fe for Mg does not significantly affect the T-x_{CO_2} conditions of the equilibria.

Wollastonite zone

The wollastonite-zone assemblage was formed by the reaction calcite + quartz = wollastonite + CO_2 and by reactions that formed grossular and vesuvianite. The net result of these reactions was nearly complete decarbonation of the argillites. Hover-Granath et al. (1983) showed schematic T-x_{CO_2} relations among the minerals in the wollastonite-zone assemblage. They assumed that the invariant point [Wo, Czo], which involves reactions among anorthite, calcite, quartz, diopside, grossular, and vesuvianite, was stable. Recent work by Hochella et al. (1982)

TABLE 3. Equilibria in calcareous argillites

Mineral formulas	
Quartz (Qtz)	SiO_2
Calcite (Cal)	$CaCO_3$
Phlogopite (Phl)	$KMg_3AlSi_3O_{10}(OH)_2$
K-feldspar (Ksp)	$KAlSi_3O_8$
Tremolite (Trem)	$Ca_2Mg_5Si_8O_{22}(OH)_2$
Diopside (Diop)	$CaMgSi_2O_6$
Wollastonite (Wo)	$CaSiO_3$
Anorthite (Anor)	$CaAl_2Si_2O_8$
Grossular (Gross)	$Ca_3Al_2Si_3O_{12}$
Vesuvianite (Ves)	$Ca_{19}Mg_2Al_{11}Si_{18}O_{69}(OH)_9$
Clinozoisite (Czo)	$Ca_2Al_3Si_3O_{12}OH$

Reaction		ln K_{eq} (2000 bars)
(Diop)	5 Phl + 6 Cal + 24 Qtz = 3 Trem + 5 Ksp + $2H_2O$ + $6CO_2$	$-65368/T + 141.14$
(Qtz)	3 Trem + 6 Cal + Ksp = Phl + 12 Diop + $2H_2O$ + $6CO_2$	$-55936/T + 126.26$
(Trem)	Phl + 3 Cal + 6 Qtz = Ksp + 3 Diop + H_2O + $3CO_2$	$-30326/T + 66.850$
(Phl, Ksp)	Trem + 3 Cal + 2 Qtz = 5 Diop + H_2O + $3CO_2$	$-28754/T + 64.369$
(Czo, Ves, Wo)	Anor + 2 Cal + Qtz = Gross + $2CO_2$	$-12609/T + 27.198$
(Czo, Ves, Cal)	Gross + Qtz = Anor + 2 Wo	$-3361.7/T + 3.9507$
(Czo, Ves, Qtz)	Anor + Wo + Cal = Gross + CO_2	$-2420/T + 9.034$
(Czo, Ves, Anor, Gross)	Cal + Qtz = Wo + CO_2	$-10189/T + 18.164$
(Qtz, Ves, Gross, Wo)	2 Czo + CO_2 = 3 Anor + Cal + H_2O	$-8074.2/T + 11.615$
(Czo, Anor, Cal)	2 Ves + 6 Qtz = 11 Gross + 4 Diop + Wo + $9H_2O$	
(Czo, Anor, Qtz)	2 Ves + 5 Wo + $6CO_2$ = 11 Gross +4 Diop + 6 Cal + $9H_2O$	
(Czo, Anor, Wo)	2 Ves + 5 Qtz + CO_2 = 11 Gross + 4 Diop + Cal +$9H_2O$	
(Anor, Wo, Ves)	2 Czo + 5 Cal + 3 Qtz = 3 Gross + H_2O + $5CO_2$	$-45939/T + 93.258$
(Anor, Wo, Cal)	5 Ves + Czo + 4 Qtz = 29 Gross + 10 Diop + $23H_2O$	
(Anor, Wo, Qtz)	3 Ves + $14CO_2$ = 9 Gross + 6 Diop + 5 Czo + 14 Cal + $11H_2O$	
(Anor, Wo, Gross)	3 Ves + $87CO_2$ = 11 Czo + 87 Cal + 9 Qtz + 6 Diop + $8H_2O$	
(Czo, Qtz, Wo)	2 Ves + $11CO_2$ = 6 Gross + 4 Diop + 5 Anor + 11 Cal + $9H_2O$	

and Valley et al. (1985) has shown that the stable invariant point is [Wo, Anor]; that is, vesuvianite forms at low temperatures from the assemblage clinozoisite + calcite + quartz rather than anorthite + calcite + quartz. The reactions among diopside-bearing calc–aluminum silicates are shown in Figure 2. All vesuvianite-absent reactions were calculated from the equilibrium-constant expressions of Rice (1983) and the fugacity coefficients of Kerrick and Jacobs (1981). The positions of reactions involving vesuvianite in Figure 2 are constrained by the reaction 2 vesuvianite + 6 quartz = 11 grossular + 4 diopside + wollastonite + $9H_2O$ (Czo, Anor, Cal), which occurs at 400 °C, 2 kbar, and $x_{CO_2} = 0$ (Hochella et al., 1982), and the topology of the vesuvianite-absent reactions. The formula $Ca_{19}Mg_2Al_{11}Si_{18}O_{69}(OH)_9$, determined by Valley et al. (1985), was used to balance the reactions. All the reactions are listed in Table 3.

The fluid compositions listed in Table 1 for wollastonite-zone assemblages, calculated from the equilibrium (Czo, Ves, Qtz) in Table 3, are generally low in x_{CO_2}. The values in many cases are, however, inconsistent with the stability of wollastonite because the plagioclase is very albitic, requiring a long extrapolation from the end-member reaction. The value of x_{CO_2} is estimated instead by the stability of the mineral assemblage. The wollastonite-zone assemblage, wollastonite + vesuvianite + grossular + diopside + calcite, is univariant in the CaO-Al_2O_3-MgO-SiO_2-CO_2-H_2O system at $P_{fluid} = P_{solid} = 2000$ bars. The reaction among these minerals, listed as (Czo, Anor, Qtz) in Table 3, is constrained to lie at a value of x_{CO_2} of about 0.0015 by the intersection of the wollastonite + calcite + quartz equilibrium and the reaction (Czo, Anor, Cal), investigated by Hochella et al. (1982). The reaction is probably nearly vertical in Figure 2 because the high-temperature side of the reaction, the side that releases the greater number of moles of a volatile component, is grossular + diopside + calcite. Thus, the reaction curve must have a negative slope and must be asymptotic to the temperature axis. An absolute error on the x_{CO_2} value cannot be determined, but even a 10% error in ln f_{CO_2} does not increase the value to more than 0.002. This value is used as the estimate of x_{CO_2} in the wollastonite zone.

The actual wollastonite-zone assemblage has a higher variance than the simplified system. Both grossular and vesuvianite contain substantial Fe_2O_3 and TiO_2 (Table 2). Fe^{3+} is strongly partitioned into the garnet; the $K_D = (X_{Fe^{3+}}/X_{Al})^{gross}/(X_{Fe^{3+}}/X_{Al})^{ves}$ is about 3.5. The effect of Fe^{3+} in these minerals is to extend the stability field of garnet to even more water-rich conditions than those shown in Figure 2. Ti is more strongly partitioned into vesuvianite; the $K_D = (X_{Ti}/X_{Al})^{gross}/(X_{Ti}/X_{Al})^{ves}$ is about 0.4. This partitioning extends the stability field of vesuvianite to more CO_2-rich conditions than shown in Figure 2. The effects of the partitioning of TiO_2 and Fe_2O_3 between grossular and vesuvianite on x_{CO_2} tend to cancel.

The transition from the diopside zone to the wollas-

tonite zone is abrupt. There is little evidence to indicate which reactions resulted in the formation of grossular and vesuvianite. The textural evidence for the sequence of mineral growth, described by Hover-Granath et al. (1983), is complex. The plagioclase in the diopside-zone assemblages is generally very anorthitic, whereas the wollastonite-zone plagioclase is albite. There is, however, no evidence for the formation of clinozoisite as predicted by the T-x_{CO_2} diagram. The transition appears to represent a distinct change in x_{CO_2} from that of the diopside zone (0.024) to that of the wollastonite zone (<0.002). The transition also represents a substantial amount of decarbonation. Thus, the wollastonite isograd is considered to be a discontinuity, an infiltration front, at which the argillites were totally recrystallized.

The mass balance

The fluids that were in equilibrium with the argillites in the Big Horse Limestone Member were nearly uniformly H_2O-rich, particularly in the wollastonite zone where the mineral assemblage indicates that the fluid composition was near $x_{CO_2} = 0.002$. The metamorphic reactions, however, were generally decarbonation reactions. Labotka et al. (1988) have shown that the CO_2/CaO wt% ratio decreased from the value for calcite (0.78) in unmetamorphosed rocks to nearly 0.00 in wollastonite-zone rocks. The decrease in this ratio occurred discontinuously, with major changes at the diopside and wollastonite isograds and little change between the isograds. Labotka et al. (1988) have also shown that, with the exception of CO_2, there was no change in the major-element chemistry during metamorphism. It is possible, then, to calculate the amount of CO_2 evolved by the rock because the mineralogy of the protolith as well as of the metamorphic rock is known.

The unmetamorphosed argillites contain calcite, quartz, plagioclase, and some combination of K-feldspar, biotite, muscovite, and chlorite. In some rocks, the minerals were probably produced by very low grade metamorphic reactions; in others, they are detrital minerals. The protolith assemblage is taken to be either calcite + quartz + muscovite + chlorite + phlogopite or calcite + quartz + muscovite + phlogopite + K-feldspar. These are common assemblages in very low grade, "biotite-zone" rocks (Labotka and Nabelek, 1986; Ferry, 1984). This assumption eliminates from consideration the biotite-forming reactions, about which little is known in these rocks.

The diopside-zone assemblage is considered to be calcite + quartz + diopside + K-feldspar + calcic plagioclase. Many diopside-zone rocks contain phlogopite or tremolite in addition, indicating that the diopside- and K-feldspar–forming reactions did not go to completion. In these cases, the mass-balance calculations determine the maximum amounts of CO_2 and H_2O that could have been released by the samples. The plagioclase is represented by the separate components albite and anorthite.

The mass balance is calculated by conserving the amount of cations, except H and C, per kilogram of the metamorphic rock. The mass-balance relation is $\mathbf{y} = \mathbf{Ax}$, in which $\mathbf{y}$ is the composition of a rock, $\mathbf{A}$ is a matrix of the compositions of the constituent minerals, and $\mathbf{x}$ is the abundance of the minerals. The solution of this equation is exact if the number of minerals equals the number of components or if the abundances ($\mathbf{x}$) are known; otherwise, the solution gives the least-squares solution. Complete details about this calculation are given in Labotka et al. (1984). The results, given in Table 4, are expressed as a mass transfer of minerals in grams per kilogram of the protolith. Table 4 indicates the grams of minerals consumed and produced during metamorphism. The resulting relation, protolith → metamorphic rock, is balanced for H_2O and CO_2. These are the net amounts of H_2O and CO_2 released by the rock. This mass-balance method calculates the total amounts of volatiles released and was used in preference to measuring the progress of individual reactions because the thin sections of coarse-grained rocks are unrepresentative of the bulk and because the mass balance is indicative of the total amount of evolved fluid, integrated over the entire period of metamorphism.

Table 4 shows the amount of CO_2 and H_2O evolved by wollastonite-zone and diopside-zone rocks. On the average, wollastonite-zone rocks evolved 158 ± 45 g (3.6 ± 1.0 mol) of CO_2 and 10.1 ± 2.7 g (0.6 ± 0.2 mol) of H_2O per kilogram of protolith. The change in mineralogy and loss of volatiles were accompanied by a reduction in solid volume of 24% ± 6%. The volume of the released volatiles was about 73% ± 20% of the starting rock volume. This was calculated assuming specific volumes of H_2O and CO_2 equal to 1.5 and 1.6 cm^3/g, respectively, which are appropriate for a temperature of about 500 °C and a pressure of 2 kbar (Burnham et al., 1969; Shmonov and Shmulovich, 1974). The diopside-zone rocks had evolved 45 ± 23 g (1.0 ± 0.5 mol) of CO_2 and 16 ± 7 g (0.9 ± 0.4 mol) of H_2O per kilogram of protolith with a $\Delta V_{solid} = -7\% \pm 4\%$.

Metamorphism resulted in a substantial loss in solid volume; some rocks had lost nearly one-third their original volume! The rocks also evolved a large quantity of CO_2 and H_2O, having an average composition of $x_{CO_2} = 0.86$ for wollastonite-zone rocks and $x_{CO_2} = 0.53$ for diopside-zone rocks. There is no systematic loss of volatiles within either zone. The amount of released volatiles is generally correlated to the amount of calcite in the protolith (Labotka et al., 1988). The principal loss of CO_2 and H_2O appears to have occurred at the isograds.

Although metamorphism resulted in a net loss of both CO_2 and H_2O, the wollastonite-zone rocks appear to have lost less H_2O than the diopside-zone rocks. This implies that a small amount of H_2O was added to wollastonite-zone rocks. At the diopside isograd, where phlogopite broke down to diopside + K-feldspar, an average of 1.0 mol of CO_2 and 0.9 mol of H_2O were evolved per kilogram of protolith, resulting in a solid-volume loss of 7%. At the wollastonite isograd, where calcite and quartz reacted to form wollastonite and where grossular and ve-

TABLE 4. Mass balance (grams per kilogram of protolith)

Sample	Qtz	Cal	Chl	Musc	Phl	Ksp	Anor	Diop	Wo	Gross	Ves	CO_2	H_2O	ΔV_{solid}*	V_{gas}**
Wollastonite zone															
80	−236	−286	0	−69	−154	151	0	225	134	61	39	126	9	−19	58
84	−276	−400	−61	−68	−56	85	0	198	249	116	25	176	13	−26	83
36	−213	−240	0	−71	−165	160	0	241	69	57	48	106	9	−17	50
37	−254	−405	−114	−117	0	82	−13	191	158	107	172	178	15	−28	85
89	−248	−390	−71	−51	−3	38	0	133	282	83	45	171	10	−25	80
98	−233	−320	0	−45	−99	98	0	145	243	37	29	141	6	−20	63
86	−306	−472	−89	−51	−17	47	0	185	335	84	63	208	13	−30	96
40	−304	−505	−71	−16	0	11	−34	119	420	48	104	222	7	−30	100
39	−242	−256	0	−162	−179	241	0	251	10	61	139	112	11	−19	54
87	−194	−205	0	−66	−173	161	0	250	25	31	72	90	8	−15	43
100	−285	−473	−75	−17	0	12	−64	140	351	170	23	208	10	−31	95
⟨x⟩	−254	−359	−44	−67	−77	99	−10	189	207	78	69	158	10	−24	73
σ	36	103	44	42	78	73	21	49	138	41	49	45	3	6	20
Diopside zone															
47	−59	−71	−78	−102	55	35	111	67	0	0	0	31	12	−5	19
137	−47	−51	−43	−124	37	62	108	26	0	0	0	22	10	−3	14
56	−41	−54	−72	−87	64	18	96	41	0	0	0	24	10	−4	15
44	−179	−182	−125	−167	−7	121	186	249	0	0	0	80	24	−13	46
135	−141	−128	−43	−184	−50	162	155	156	0	0	0	56	16	−9	32
54	−112	−126	−120	−296	109	134	266	67	0	0	0	56	24	−8	36
⟨x⟩	−97	−102	−80	−160	35	89	153	101	0	0	0	45	16	−7	27
σ	57	52	36	76	56	58	65	86	0	0	0	23	7	4	13

Note: Grams lost (−) or gained (+) per kilogram of protolith during the mass transfer protolith → metamorphic rock. Mean = ⟨x⟩ and standard deviation = σ.

* Percent of the protolith solid volume lost.

** Percent of the solid volume. Calculated with specific volumes of 1.5 and 1.6 mL/g for H_2O and CO_2, respectively.

suvianite formed by reactions among anorthite, calcite, wollastonite, and diopside, an additional 2.6 mol of CO_2 per kilogram of protolith was released and 0.3 mol of H_2O per kilogram of protolith was added to the rock on average, resulting in a further volume reduction of 17% of the original volume.

INFILTRATION

The composition of the volatile fraction evolved by the argillites during metamorphism was significantly different from the equilibrium fluid composition indicated by the mineral assemblages. A water-rich fluid must have infiltrated the argillites to dilute the CO_2-rich fluid evolved by the rocks. The amount of fluid that infiltrated the argillites can be estimated by balancing the evolved fluid with sufficient H_2O to obtain the equilibrium composition. This procedure, described by Ferry (1980, 1986) for rocks undergoing fluid-composition–buffering reactions, can be written as

$$w_{CO_2} = \frac{m_{CO_2,e}}{m_{CO_2,e} + m_{H_2O,e} + m_{H_2O,i}} \quad (1)$$

in which w_{CO_2} is the weight fraction of CO_2, m is the mass of volatile component in grams per kilogram of protolith, the subscript e refers to evolved volatiles (or, if negative, added), and the subscript i refers to infiltrated volatiles. Equation 1 is independent of the amount of initial pore fluid because the composition remains constant. The equation is accurate if every increment of infiltrating H_2O causes an incremental advance in the volatilization reactions, thereby maintaining a constant fluid composition.

The amount of decarbonation and dehydration that the diopside-zone samples have undergone (Table 4) at a fluid composition of $x_{CO_2} = 0.024$ ($w_{CO_2} = 0.057$) requires that 730 ± 360 g of H_2O per kilogram of rock have infiltrated this zone. The amount that infiltrated the wollastonite isograd depends on the x_{CO_2} that prevailed at the isograd. The value of x_{CO_2} within the zone was 0.002, but the value at which the reaction occurred must have been higher. As described in a following section, a value of 0.004 is adopted as the value at the isograd. The nearly complete decarbonation at the wollastonite isograd, where an additional 113 ± 50 g of CO_2 per kilogram of protolith was lost and 6 ± 8 g of H_2O per kilogram of protolith was gained at a fluid composition of $x_{CO_2} \geq 0.002$ ($w_{CO_2} \geq 0.005$) requires an infiltration of as much as 22.5 ± 9 kg of H_2O per kilogram of protolith. If the value of x_{CO_2} was 0.004 at the isograd, then the infiltrated amount was 11.2 ± 5 kg per kilogram of protolith. These values, representing water/rock ratios (by weight) of 0.73 in the diopside zone and 11.9 to 23.2 in the wollastonite zone integrated over the entire time of metamorphism, are phenomenal. Allowing for the greatest possible error in the equilibrium fluid composition within the wollastonite zone—$x_{CO_2} = 0.01$ based on wollastonite stability—the water/rock ratio by weight still had to be 4.6.

The calculated water/rock ratios are so large that it is worth considering other evidence for massive infiltration of H_2O. One implication of the mass balance is the large loss in solid volume during metamorphism, ~25% in the

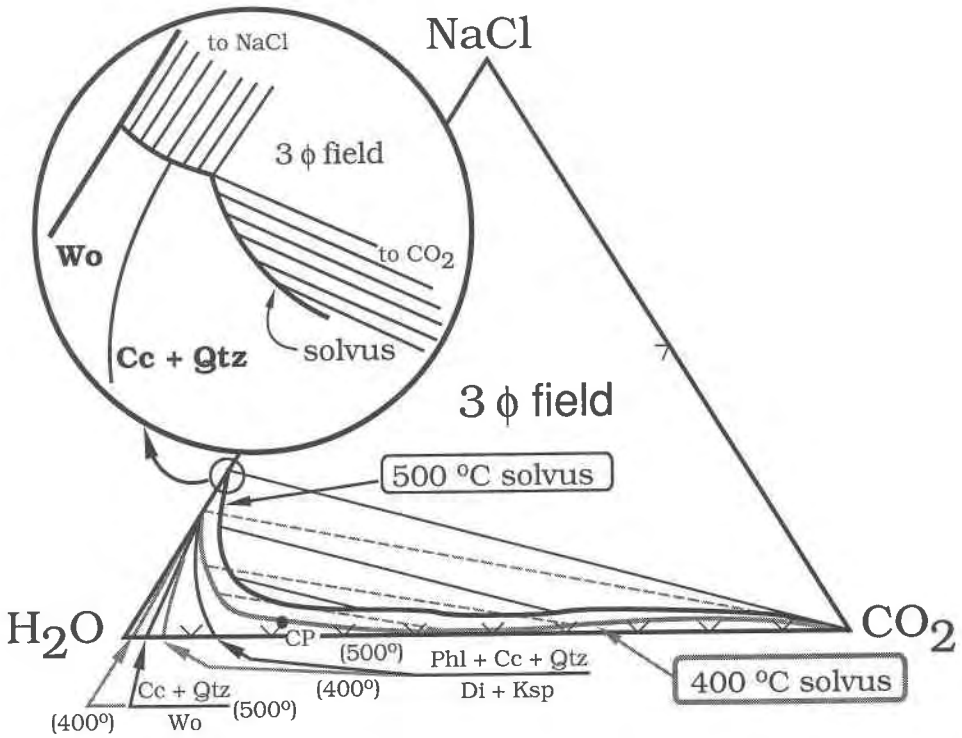

Fig. 3. Isothermal, isobaric phase diagram for NaCl-H_2O-CO_2 showing the solvus at 500 (black line) and 400 °C (gray line), 2000 bars. The critical point is indicated on the 400 °C solvus as CP. Curves showing the stability limits of calcite + quartz and phlogopite + calcite + quartz for the two temperatures are also projected onto the diagram. The curves for 500 °C are black; those for 400 °C are gray. These reaction curves are asymptotic to the NaCl-H_2O side of the diagram and intersect the solvus at halite saturation. The enlargement shows the nature of this intersection for the calcite + quartz = wollastonite reaction schematically. The fugacity coefficients of Bowers and Helgeson (1983a) were used to calculate the solvi and the positions of the reactions.

wollastonite zone. We have been unable to document this large ΔV by mapping individual layers; however, several deformation features indicating a change in volume have been noted. Near the contact with the stock, the country rocks are cut by numerous veins, now filled with grossular and vesuvianite, and sills of granite, which indicate that the rock was fractured during metamorphism. In addition, the country rocks along the margins of the stock are locally ductilely deformed, indicating that some of the solid volume loss created during reaction may have been occupied by the intrusion.

The $\delta^{13}C$ data of Nabelek et al. (1984) indicate that, in general, decarbonation took place fractionally; that is, the evolved CO_2 was removed from the rock as it was being generated. The implication of this process is that x_{CO_2} in the infiltrating fluid phase was 0.0. The mineral assemblages are consistent with a nearly pure H_2O fluid phase, and if a large volume of H_2O were infiltrating the wollastonite zone, the evolved CO_2 would have readily been removed. The water/rock ratio indicated by the O-isotope data for wollastonite-zone rocks is only 10% to 30% of that indicated by the mineral assemblages. The difference reflects either incomplete isotope exchange between the infiltrating H_2O and the rock or a difference between the water/rock ratio measured by the mineral assemblage and the integrated fluid flux. Labotka and Nabelek (1987) showed that the degree of isotope exchange was aided by the amount of volatilization. The discrepancy in the water/rock ratios determined by the isotope study and by this study probably indicates differences in the processes recorded by the rocks.

The values of infiltrated H_2O are calculated by assuming that local equilibrium is maintained during infiltration. Nonequilibrium processes, for example, exsolution and escape of a CO_2-rich vapor from the fluid phase, can have significant consequences on the calculated water/rock ratios. A small amount of NaCl disolved in the fluid significantly expands the immiscibility region between H_2O-rich and CO_2-rich phases (Bowers and Helgeson, 1983a). The two-phase fluid can be fractionated efficaciously by escape ("boiling off") of the less-dense CO_2-rich phase. Trommsdorff and Skippen (1986) argued that this process can lead to halite saturation in the small proportion of residual H_2O-rich liquid. Bowers and Helgeson (1983b) showed that many mixed-volatile reaction surfaces intersect the H_2O-CO_2 solvus at geologically significant temperatures with the addition of very little NaCl to the fluid. Figure 3 shows the H_2O-CO_2-NaCl phase

TABLE 5. Progressive metamorphism of NP 18H-89, a model for the Big Horse Limestone Member

	Wollastonite-zone assemblage		High diopside–zone assemblage		Low diopside–zone assemblage		Nascent diopside–zone assemblage		Unmetamorphosed assemblage	
Mineral	wt%	mode	wt%	mode	wt%	mode	wt%	mode	wt%	mode
Quartz	0.00	0.0	15.98	16.5	16.68	17.1	21.56	22.2	24.78	25.5
Calcite	20.78	20.8	50.57	50.7	52.11	52.2	56.17	56.3	59.76	59.9
Muscovite	0.00	0.0	0.00	0.0	0.00	0.0	0.00	0.0	5.13	5.1
Chlorite	0.00	0.0	0.00	0.0	0.00	0.0	0.00	0.0	7.12	6.5
Phlogopite	0.00	0.0	0.00	0.0	0.00	0.0	5.65	5.5	0.28	0.3
Anorthite	0.00	0.0	7.52	7.4	7.14	7.1	7.14	7.1	0.00	0.0
Tremolite	0.00	0.0	0.00	0.0	4.13	3.7	4.13	3.7	0.00	0.0
Diopside	13.33	11.3	14.01	11.9	8.79	7.5	0.00	0.0	0.00	0.0
Wollastonite	28.22	26.5	0.00	0.0	0.00	0.0	0.00	0.0	0.00	0.0
Grossular	8.28	6.3	0.00	0.0	0.00	0.0	0.00	0.0	0.00	0.0
Vesuvianite	4.51	3.7	0.00	0.0	0.00	0.0	0.00	0.0	0.00	0.0
K-feldspar	3.77	4.0	3.77	4.0	3.77	4.0	0.00	0.0	0.00	0.0
Albite	1.59	1.6	1.59	1.6	1.59	1.6	1.59	1.6	1.59	1.6
Sphene	0.58	0.5	0.58	0.5	0.58	0.5	0.58	0.5	0.58	0.5
Apatite	0.75	0.6	0.75	0.6	0.75	0.6	0.75	0.6	0.75	0.6
Sum	81.82	75.4	94.78	93.2	95.54	94.4	97.58	97.6	100.00	100.0
Solid density	2.96		2.78		2.74		2.73		2.73	
	Cumulative loss of volatiles (grams per kilogram of protolith)									
CO_2 loss	171.4		40.4		33.6		15.8			
H_2O loss	10.4		11.7		10.8		8.3			
	Cumulative difference in specific enthalpy (joules per kilogram of protolith)									
ΔH	332 544		105 317		91 022		54 196			

Note: Wt% indicates weight percent of protolith (i.e., unmetamorphosed assemblage).

diagram at 2 kbar, 400 and 500 °C, calculated from the data of Bowers and Helgeson (1983a), and the positions of the equilibria calcite + quartz = wollastonite + CO_2 and phlogopite + 3 calcite + 6 quartz = K-feldspar + 3 diopside + $3CO_2$ + H_2O, calculated with the fugacity coefficients of Bowers and Helgeson (1983a). Both equilibria, which caused major decarbonation of the Big Horse Limestone Member, are asymptotic to the H_2O-NaCl side of the triangle and fail to intersect the solvus between the two fluid phases. Although infiltration of a saline solution could have caused separation of an initially CO_2-rich pore fluid, this would have occurred before decarbonation. Even under NaCl-saturated conditions, the major decarbonation reactions occurred in the one-phase, H_2O-rich region, and no separation of a CO_2-rich phase could have occurred. If there was a substantial amount of dissolved salts in the infiltrating fluid, then the calculated water/rock ratios are minimal values because the equilibrium value of x_{CO_2} decreases to zero and substantially more H_2O had to have infiltrated the rock.

T-x_{CO_2}-$m_{H_2O,i}$ PATH OF METAMORPHISM

A representative sample

The conclusion is inescapable: the wollastonite zone in the Big Horse Limestone Member interacted with vast quantities of an H_2O-rich fluid. The percolation was, no doubt, abetted by the substantial loss in solid volume, which certainly enhanced permeability. The large water/rock ratio resulted from the effect of confining the water in the reactive layers. The intervening limestone layers were essentially impermeable.

The results are impressive, but they might not be reasonable. It should be possible to place quantitative limits on the fluid and heat fluxes over the lifetime of the aureole, based on a simple physical model for heat and mass transport. The physical model must be simple because many parameters—like the amount of released CO_2, fluid composition, ΔV_{solid}, and ∇T—depend on the rock composition and the geometry of the aureole. The carbonate rocks have a range in composition, and the geometries of the stock and country rock are irregular. For simplicity, one rock composition, that of 18H-89, is chosen to represent the carbonate rock composition. The composition of this sample (Table 2 in Labotka et al., 1988) is close to the average, and the mass balance (Table 4) indicates that the amounts of evolved CO_2 and H_2O were also near the average of the analyzed samples.

Table 5 shows the changes in the mode of this sample with progressive metamorphism. The protolith contained the assemblage calcite + quartz + chlorite + muscovite + biotite + albite. Breakdown of chlorite and muscovite by reactions like muscovite + chlorite + calcite + quartz = phlogopite + anorthite + CO_2 + H_2O, and chlorite + calcite + quartz = tremolite + anorthite + CO_2 + H_2O produced the first recognizable metamorphic assemblage. There was little loss in solid volume and minor production of CO_2 and H_2O at this point. Diopside and K-feldspar joined the assemblage by the fluid-composition–buffering reactions among all these minerals, as described in the previous section on fluid composition. These reactions proceeded until phlogopite and tremolite were consumed and accounted for a small loss in solid volume

and the release of about 30 g of CO_2 and H_2O per kilogram of protolith in the molar ratio of $x_{CO_2} = 0.75$. Field evidence is insufficient to resolve the first appearance of tremolite + phlogopite from the first appearance of diopside + K-feldspar. In this simplified model, the first appearance of tremolite + phlogopite coincides with the inception of reactions producing diopside + K-feldspar.

After phlogopite and tremolite were consumed, wollastonite, vesuvianite, and grossular were produced by reactions like calcite + quartz = wollastonite + CO_2, anorthite + calcite + quartz = grossular + CO_2, and anorthite + diopside + calcite + quartz + H_2O = vesuvianite + CO_2. This step resulted in a quartz-free and nearly calcite-free assemblage with a volume loss of about 25%, the release of 131 g of CO_2 per kilogram of protolith and absorption of 1.3 g of H_2O per kilogram of protolith. Although the final assemblage appears to be isobarically univariant, the substantial amounts of Fe and Ti in the grossular and vesuvianite increase the variance. The wollastonite-zone reactions are presumed to go to completion at the wollastonite isograd.

The diopside zone

The most appropriate T-x_{CO_2} path of metamorphism for the model is difficult to choose. As described above, the diopside-zone samples contain assemblages that fall on either side of the isobaric invariant point calcite + quartz + tremolite + diopside + phlogopite + K-feldspar, and some samples contain the invariant assemblage (Table 1). The range in temperature within the diopside zone is small—zero, within the errors—indicating near–invariant-point conditions. Rice and Ferry (1982) have suggested that many isograds represent invariant assemblages, particularly in those terranes that are "rock-dominated." In the Big Horse Limestone Member, the entire diopside zone seems to represent invariance. The occurrence of invariant assemblages implies that the initial temperature at the isograd was lower than that of the invariant point, but very little reaction was required to buffer the fluid composition to that of the invariant point (see above). It is only at the invariant point that significant reaction can occur, as described by Rice and Ferry (1982), resulting in a noticeable change in mineralogy. However, the invariant assemblage itself is incapable of buffering the fluid composition at that of the invariant point. All the reactions release CO_2 and H_2O in the ratio 3:1. The only reaction that can occur, in the absence of infiltration, is the fluid-absent reaction tremolite + K-feldspar = phlogopite + 2 diopside + 4 quartz. Infiltration of an H_2O-rich fluid, however, drives decarbonation reactions to maintain the fluid composition at that of the invariant point.

The nascent diopside-zone assemblage formed from the breakdown of muscovite and chlorite in the incipiently metamorphosed (or unmetamorphosed) rocks. The reactions responsible for the disappearance of these minerals must have occurred at x_{CO_2} conditions near 0.024, the value at the invariant point. Each kilogram of protolith released 15.8 g of CO_2 and 8.3 g of H_2O (Table 5), requiring infiltration of 234 g of H_2O per kilogram of protolith to maintain the fluid composition at $x_{CO_2} = 0.024$.

After these reactions went to completion, the rock consisted of calcite + quartz + tremolite + phlogopite + calcic plagioclase, and continued reaction among these minerals produced diopside + K-feldspar. Under equilibrium conditions, an invariant assemblage can only occur at an isograd, not within a wide zone. This is because there can be no heat or fluid flux across the isograd until one of the minerals is consumed. The diopside isograd, then, is represented by the invariant assemblage.

The invariant-point reactions can be represented by the two linearly independent reactions phlogopite + 3 calcite + 6 quartz = K-feldspar + 3 diopside + $3CO_2$ + H_2O (Reaction I) and tremolite + K-feldspar = phlogopite + 2 diopside + 4 quartz (Reaction II). Figure 4 shows the possible progress of these two reactions for the bulk composition of 18H-89 on a ξ_I-ξ_{II} plot (Thompson et al., 1982; Rice and Ferry, 1982). The origin represents the incipient isograd assemblage calcite + quartz + tremolite + phlogopite in the proportions shown in Table 5. The diopside zone represents a traverse from the origin in Figure 4 to the farthest corner. For the two reactions (I and II) representing the invariant point, water/rock ratio (W/R) isopleths are nearly parallel to isenthalps. Gradients in the heat and fluid fluxes are, therefore, nearly parallel, and regardless of the relative proportion of the fluxes, reactions must proceed in a nearly horizontal direction on the ξ_I-ξ_{II} plot. The diopside isograd is represented by the horizontal traverse across the plot from the origin to the limit (phlogopite). This traverse required an infiltration of 294 g of H_2O and an addition of 36800 J of heat per kilogram of protolith.

The diopside zone is represented by the univariant assemblage calcite + quartz + tremolite + diopside + K-feldspar. The diopside zone persisted until tremolite was consumed, when the assemblage no longer buffered the fluid composition. Within this zone, temperature and fluid composition are related by the equilibrium constant for the reaction tremolite + 3 calcite + 2 quartz = 5 diopside + $3CO_2$ + H_2O (Reaction III):

$$3\ln f_{CO_2} + \ln f_{H_2O} = -28754/T + 64.369, \qquad (2)$$

where

$$f_{CO_2} = x_{CO_2}\gamma_{CO_2}f^0_{CO_2} \qquad (3)$$

and

$$x_{CO_2} = 3\xi_{III}/(4\xi_{III} + m_{H_2O,i}/M_{H_2O}), \qquad (4)$$

where $m_{H_2O,i}$ = mass of infiltrated H_2O and M_{H_2O} = molecular weight of H_2O.

This set of equations can be represented in general form as $f(T) = g(x, m^i_{H_2O})$; therefore, only if the heat or mass flux is known can the reaction progress be calculated. A simple constraint and an additional assumption, however, allow the T-x_{CO_2} path to be determined. The con-

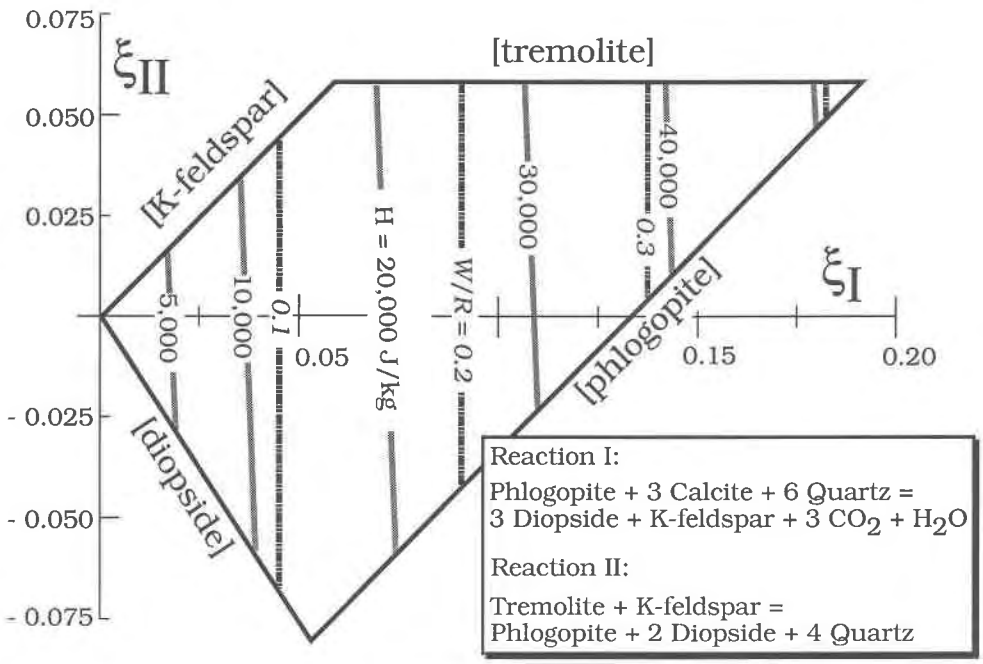

Fig. 4. The reaction space for the diopside-isograd invariant assemblage. A fluid-present (I) and a fluid-absent (II) reaction are necessary and sufficient to describe the abundances of minerals within the given bulk composition of sample NP 18H-89. The diagram is limited within the bulk composition by the disappearance of one phase. The phase that disappears at a boundary is indicated in brackets. The only reaction that can occur along a boundary is the one indicated by the absent phase. These reactions are given in Table 3. The contours indicate the amount of heat (L) required by the reaction progress (shaded lines) and the amount of H_2O required to maintain constant fluid composition (broken lines) per kilogram of protolith. The contours are given by

$$x_{CO_2} = 0.024 = \frac{3\xi_I}{4\xi_I + m_{H_2O,i}/M_{H_2O}}$$

$$L = \Delta H_I \xi_I + \Delta H_{II} \xi_{II} = 272\,782\xi_I + 12972\xi_{II}.$$

M_{H_2O} is the molecular weight of H_2O, $m_{H_2O,i}$ is the mass of infiltrated H_2O, and ΔH is the enthalpy of reaction. These are nearly parallel, indicating that in the presence of thermal and fluid-pressure gradients, advancement through the diagram is nearly horizontal, i.e., in the direction of increasing ξ_I.

straint is to consider the mineral assemblage to be in equilibrium with only the fluid that was in the pore space created at the diopside isograd. Any fluid that was generated by Reaction III or that infiltrated the diopside zone displaced and consequently diluted the pore fluid. The volume of the pore space is presumed to have been constant; that is, significant deformation did not occur until after metamorphism when fluid generation ceased and pore pressures were reduced to lithostatic or lower values. The additional assumption is that fluid infiltration was a uniform process so that the ratio between $m_{H_2O,i}$ and ξ was constant, as it is in strictly isothermal infiltration in which x_{CO_2} is constant.

The constant-volume constraint can be represented by

$$y'_{CO_2} = [3v_{CO_2}\Delta\xi_{III} + (V - 3v_{CO_2}\Delta\xi_{III} - v_{H_2O}\Delta\xi_{III} - \Delta v_{H_2O,i})y_{CO_2}]/V \quad (5)$$

in which y_{CO_2} is the volume fraction of CO_2, y'_{CO_2} is the volume fraction after incremental reaction progress $\Delta\xi_{III}$ and incremental influx of a volume of H_2O $\Delta v_{H_2O,i}$, v is the molar volume, and V is the constant volume of the pore space. Labotka et al. (1984) showed that for infinitesimal processes, Equation 5 can be integrated if $\Delta v_{H_2O,i} = v_{H_2O,i}\Delta\xi$ is is the second assumption. The result is

$$\xi = \frac{V}{3v_{CO_2} + v_{H_2O} + v_{H_2O,i}} \cdot \ln\left(\frac{3v_{CO_2} - (3v_{CO_2} + v_{H_2O} + v_{H_2O,i})y^0}{3v_{CO_2} - (3v_{CO_2} + v_{H_2O} + v_{H_2O,i})y}\right). \quad (6)$$

The volume fraction is related to the mole fraction, assuming ideal mixing, by

$$y_{CO_2} = \frac{x_{CO_2}}{x_{CO_2} + (1 - x_{CO_2})(v_{H_2O}/v_{CO_2})}. \quad (7)$$

The initial value $y^0_{CO_2}$, that of the invariant point, was 0.061, which corresponds to $x_{CO_2} = 0.024$. Specific volumes of CO_2 and H_2O were taken to be 1.63 and 1.50 mL/g, respectively (Shmonov and Shmulovich, 1974; Burnham et al., 1969). The porosity was 5.6% (22 mL per kilogram of protolith), which represents the solid-volume loss after the conversion of the protolith to the

incipient diopside-isograd assemblage and after the consumption of phlogopite in the invariant assemblage (Table 5). The diopside zone terminated where tremolite was consumed by Reaction III. The value of ξ_{III} at that point was 0.051.

The composition of the fluid and, therefore, the temperature at the limit of the diopside zone can be calculated from Equation 5 with the assumption of a value for $v_{H_2O,i}$. Limits on the volume of infiltrating fluid are 3267 mL/ξ for isothermal infiltration (calculated from Eq. 4 with $x_{CO_2} = 0.024$) and 0 for a closed system. The calculated fluid composition at the limit of the diopside zone, then, must fall within the range $x_{CO_2} = 0.024$ to $x_{CO_2} = 0.212$. The only way of determining the proper value of $v_{H_2O,i}$ is by knowing the value of x_{CO_2} at the high-temperature limit of the diopside zone. This value must be near 0.024, certainly not greater than 0.05 (Table 1), but it is not known precisely. The diopside isograd required 234 g of infiltrated H_2O per kilogram of protolith to break down chlorite and muscovite plus 294 g per kilogram of protolith to break down phlogopite. Because the amount of decarbonation that occurred within the diopside zone was only about 15% of the total decarbonation at this point, the amount of infiltrating water was arbitrarily chosen as 100 mL per kilogram of protolith (equivalent to 1915 mL/ξ). If this amount of water interacted with the rocks in the diopside zone, a fluid would have been produced having a composition of $x_{CO_2} = 0.04$.

The temperature at this composition would have been 464 °C (from Eq. 2). These results are consistent with the observed temperature and fluid composition. At the maximum reasonable value for x_{CO_2} of 0.05, indicated by values in Table 1, the error in the temperature at the limit of the diopside zone is only 2 °C, and the error in the amount of infiltrated fluid is only 25 mL per kilogram protolith.

The integrated water/rock ratio in the diopside zone for this representative rock would have been about 0.59, derived from the amount of H_2O required to break down chlorite + muscovite, the amount required by the invariant assemblage, and the amount required by the continuous breakdown of tremolite within the zone. This value is consistent with the values required by the constant fluid composition described in the previous section on infiltration.

The wollastonite zone

The wollastonite isograd, although considerably more complex than the diopside isograd because of the number of reactions represented, is much simpler to model. The isograd is considered to be a discontinuity across which several reactions occurred, resulting in the wollastonite-zone assemblage wollastonite + calcite + vesuvianite + grossular + diopside + K-feldspar. The reason for this discontinuity appears to be the large quantities of H_2O that must have interacted with the Big Horse Limestone Member, as indicated by the mass-balance calculations. Although vesuvianite- and grossular-producing reactions are involved, major recrystallization of the rock occurred by the reaction calcite + quartz = wollastonite + CO_2 (Reaction IV). The fluid composition along this reaction at a temperature of 464 °C, the high-temperature limit of the diopside zone, is $x_{CO_2} = 0.004$. This composition will be taken as the composition at the wollastonite isograd. Formation of the wollastonite-zone assemblage, resulting in the loss of 131 g of CO_2 per kilogram of protolith and absorption of 1.3 g of H_2O per kilogram of protolith (Table 5), required the infiltration of 13300 g of H_2O and 227 000 J of heat per kilogram of protolith. These values are consistent with the ranges of values observed for all wollastonite-zone rocks, as described in the previous section.

The T-x_{CO_2} path

Figure 5 summarizes the T-x_{CO_2} conditions and the mineral assemblages that are believed to be representative of the metamorphism of the Big Horse Limestone Member. The protolith contained the calcite- and quartz-bearing assemblage muscovite + chlorite + phlogopite. Within this unmetamorphosed or incipiently metamorphosed zone, the temperature was less than 434 °C, and the fluid composition was near $x_{CO_2} = 0.02$. The intergranular porosity was essentially 0. Near the diopside isograd, chlorite and muscovite broke down under the infiltration of 234 g of H_2O per kilogram of protolith to form the assemblage phlogopite + tremolite + calcic plagioclase, the T-x_{CO_2} conditions intersected the reaction (Ksp), and, with a trivial amount of reaction, the T-x_{CO_2} conditions reached those of the invariant point. The diopside isograd represented the persistence of the invariant assemblage until the reaction (Trem) consumed the available phlogopite. At this point, the porosity was about 6%, x_{CO_2} was 0.024, the temperature was 434 °C, and 528 g of H_2O per kilogram of protolith had infiltrated the Big Horse Limestone Member. The diopside zone represented the univariant assemblage tremolite + diopside + K-feldspar + calcic plagioclase. The high-temperature limit of the diopside zone was reached when tremolite was consumed, x_{CO_2} was 0.046, temperature was 464 °C, an additional 67 g of H_2O per kilogram of protolith infiltrated the rock, and the porosity had increased to 7%. Major recrystallization occurred at the wollastonite isograd. The rocks were nearly completely decarbonated resulting in the assemblage wollastonite + diopside + K-feldspar + vesuvianite + grossular, with only minor amounts of calcite. Massive infiltration occurred at this isograd; at a temperature of 464 °C and $x_{CO_2} = 0.004$, the water/rock mass ratio was about 13.3, more than twenty times greater than the ratio for diopside-zone rocks (0.59). The wollastonite isograd truly represents an infiltration front of water-rich fluid that emanated from the stock.

Fluid flow and heat advection

A fluid reservoir

There is a substantial difference between the wollastonite and diopside zones in the amount of interaction with

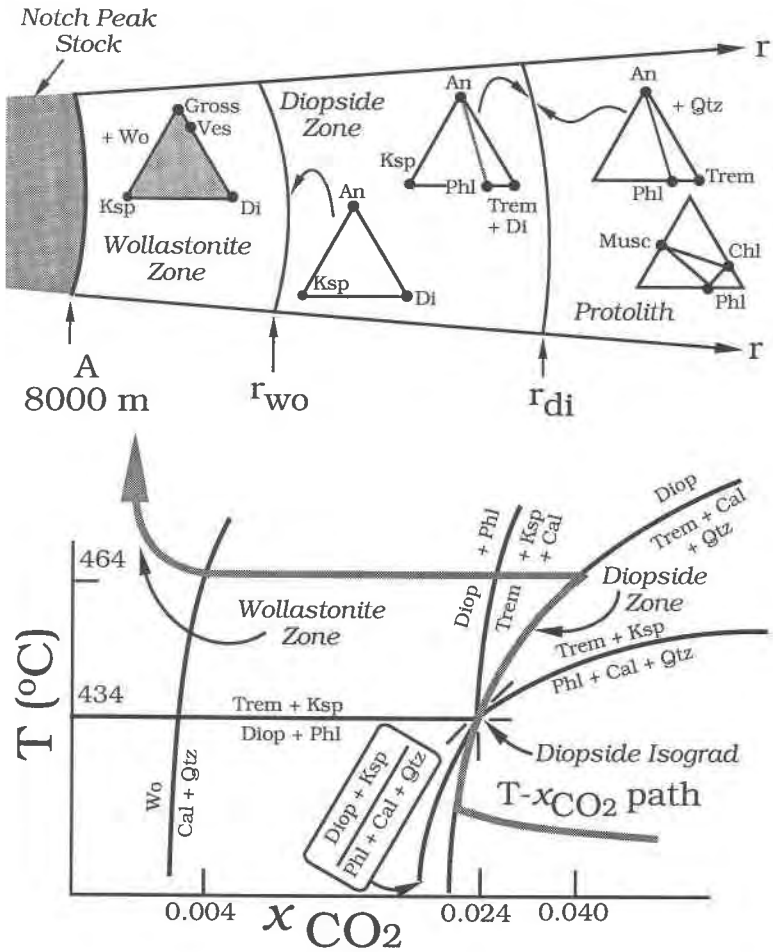

Fig. 5. Conceptualization of the T-x_{CO_2}-m_{CO_2} path of metamorphism of the calcareous argillites. The top portion shows a radial section of the aureole, divided into three zones, separated by the diopside and wollastonite isograds. A is the radius of the stock, and r is the radial distance in the model calculations, as indicated in Table 6. The assemblages in these zones are shown on an Al_2O_3-$KAlSi_3O_8$-MgO diagram, projected from calcite + quartz + H_2O + CO_2. Wollastonite-zone rocks contain wollastonite instead of quartz. At the diopside isograd, the protolith formed the nascent diopside-zone assemblage calcite + quartz + tremolite + phlogopite + calcic plagioclase. Diopside and K-feldspar joined the assemblage at the isograd. On the high-temperature side of the isograd, phlogopite disappeared. Throughout the diopside zone, tremolite + calcite + quartz continously broke down to form diopside. The wollastonite isograd represents the reaction front where wollastonite + vesuvianite + grossular formed. The T-x_{CO_2} diagram shows the path of metamorphism. The path changed from that of a fluid-composition buffer (a rock-dominated system) in the diopside zone to that of an unbuffered, fluid-dominated system in the wollastonite zone.

externally derived fluid. The fluid that infiltrated the wollastonite zone would have attained a composition of x_{CO_2} = 0.004. If the fluid that interacted with wollastonite-zone rocks infiltrated the diopside zone, then only 842 g of fluid per kilogram of protolith out of the more than 13 kg of fluid per kilogram of protolith actually interacted with the diopside-zone rocks. How can rocks on one side of the wollastonite isograd have interacted with a large volume of water, whereas the rocks on the other side have not? Clearly, little infiltrating fluid crossed the isograd, and there is no evidence for large-scale transport of water parallel to the isograd because the intervening limestone shows no effects. Vertical streaming of water probably occurred, but the most significant vertical transport probbly occurred at the roof of the stock, not along the margins. The apparent infiltration of the wollastonite zone can be realistically imagined to have occurred by the equilibration of the wollastonite-zone rocks with the large reservoir of water issuing from the crystallizing stock. As the wollastonite isograd advanced, the large change in porosity allowed the fluid near the isograd, which consisted mostly of CO_2 evolved from the Big Horse Limestone Member, to mix thoroughly with the water-rich fluid in the reservoir of the Notch Peak stock. In this case, the large water/rock ratio represents the size of the reservoir that equilibrated with the wollastonite-zone rocks, but does not represent the integrated fluid flux through the wollastonite zone.

The size of the reservoir required by a 500-m-wide wollastonite zone can be calculated from the model, as-

suming spherical geometry of the stock. The dips on the contact between the stock and the carbonate rock range from 0 to 25°, and the apparent radius of the stock is 3360 m. Using the maximum dip of 25°, which gives the most conservative estimate, the radius of the stock must be 8 km. With this radius, the ratio of the volume of the wollastonite zone to surface area of the stock is 532 m. The use of the ratio minimizes the uncertainty of the shape of the unexposed part of the stock. The amount of CO_2 evolved from the Big Horse Limestone Member in the wollastonite zone was 310 m^3/m^2, calculated from Table 5; the total amount is determined by multiplying this number by the surface area of the contact. The amount of H_2O required for a fluid composition with $x_{CO_2} = 0.004$ was 34300 m^3/m^2. The intergranular porosity of the protolith of the wollastonite zone was about 25%, corresponding to a volume of 133 m^3/m^2. The total volume of the reservoir relative to the surface area was 34500 m^3/m^2. The Big Horse Limestone Member is 220 m thick and is in contact with the stock for a distance of 9 km, but only half the unit is argillite. The affected surface area is 9.9×10^5 m^2. The required reservoir size was, therefore, 3.4×10^{10} m^3. This value represents a volumetric water/rock ratio of 64.8 for the argillite, and a weight ratio of 13.3, as required by Table 5. The volume of the stock, again assuming spherical geometry, is 2.14×10^{12} m^3, 100 times the required reservoir size. Total porosities of granitic rocks, reported by Norton and Knapp (1977), are about 4%. If the Notch Peak stock has a similar porosity, the volume of the pore space was more than sufficient to act as the reservoir for the fluid that infiltrated the Big Horse Limestone Member and, perhaps, was sufficient for the entire aureole.

The amount of water expelled from the granitic magma during crystallization can also be estimated. Nabelek et al. (1983) determined that the magma contained about 3 wt% H_2O and that about 10% of that water was incorporated into biotite and hornblende. The amount of H_2O released during crystallization, therefore, was about 1.6×10^{14} kg, or 2.9×10^{11} m^3 (at 1.77×10^{-3} m^3/kg). This is about 3 to 10 times the amount of pore space available. The expelled fluid must have been under significant pressure, and most must have escaped through the roof. The amount that interacted with the Big Horse Limestone Member was only about 10% of the total.

The water/rock ratio calculated from the mass balance does not, apparently, represent the integrated fluid flux during metamorphism, but rather the volume of the fluid reservoir with which the rocks equilibrated during metamorphism. What, then, was the fluid flux during metamorphism? The flux of fluid and heat through the Big Horse Limestone Member can be estimated from the simplified model for metamorphism and the consideration of heat and fluid transport from the stock.

Heat and fluid flow

The heat from the Notch Peak stock is considered to have been transported primarily by conduction and by advection of the fluid issuing from the crystallizing magma. The following discussion is more thoroughly developed by Bird et al. (1960), Carslaw and Jaeger (1959), Muskat (1937), and other texts on transport phenomena. The heat flux, $\mathbf{J}$, is given by

$$\mathbf{J} = -K_j \nabla T + c_{H_2O} T \mathbf{Q}, \tag{8}$$

in which K_j is the thermal conductivity, c_{H_2O} is the specific heat of water, and $\mathbf{Q}$ is the mass flux of water. The first term on the right-hand side of Equation 8 is the conductive flux, and the second is the advective flux. Conservation of energy requires

$$-(\rho_b c_b)(\partial T/\partial t) = \nabla \cdot \mathbf{J}, \tag{9}$$

which, from Equation 8, is equivalent to

$$(\rho_b c_b)(\partial T/\partial t) = \nabla \cdot K_j \nabla T - \nabla \cdot c_{H_2O} T \mathbf{Q}. \tag{10}$$

The quantity $(\rho_b c_b)$ is the product of the density and specific heat of the bulk rock-and-pore-fluid composite; it can be represented by

$$\rho_b c_b = \phi \rho_{H_2O} c_{H_2O} + (1 - \phi)\rho_r c_r, \tag{11}$$

in which ϕ is the porosity, and the subscript r refers to the rock.

Fluid flow is governed by Darcy's law in which the mass flux is proportional to the fluid-pressure gradient (∇p):

$$\mathbf{Q} = -K_q \nabla p, \tag{12}$$

in which the constant of proportionality, K_q, the hydraulic conductivity, depends on the nature of the rock and the fluid. K_q can be written as $\rho k/\eta$, in which ρ is the fluid density, η is the fluid viscosity, and k is the rock permeability. Conservation of fluid mass requires

$$-(\partial \rho_{H_2O} \phi/\partial t) = \nabla \cdot \mathbf{Q}. \tag{13}$$

The equations governing fluid flow are strictly analogous to those governing heat flow. The time derivative in Equation 13 can be expanded to give

$$\frac{\partial \rho_{H_2O} \phi}{\partial t} = \rho \frac{\partial \phi}{\partial t} + \phi \rho \beta \frac{\partial p}{\partial t} - \phi \rho \alpha \frac{\partial T}{\partial t}, \tag{14}$$

in which α is the isobaric thermal expansion of the fluid and β is the isothermal compressibility of the fluid.

The equations for flow of heat and fluid (8 and 12) can be combined with the equations of continuity (9 and 13) to give two equations that describe the temperature and fluid pressure as functions of position and time. For constant conductivities, these are

$$[\phi \rho_{H_2O} c_{H_2O} + (1 - \phi)\rho_r c_r](\partial T/\partial t) = K_j \nabla^2 T + c_{H_2O} K_q (\nabla T \cdot \nabla p + T \nabla^2 p) \tag{15}$$

and

$$\rho(\partial \phi/\partial t) + \phi \rho \beta (\partial p/\partial t) - \phi \rho \alpha (\partial T/\partial t) = K_q \nabla^2 p. \tag{16}$$

In general, there are no solutions to this set of nonlinear equations in closed form. Analytic solutions have been

TABLE 6. Constants and field equations for fluid and heat transport in the Big Horse Limestone Member

Symbol	Description	Value	Source*
A	Radius of the Notch Peak stock (m)	8000	
α	Thermal expansion of water (K^{-1})	1.51×10^{-3}	2
β	Compressibility of water (MPa^{-1})	1.45×10^{-4}	2
c	Specific heat, diopside-zone and unmetamorphosed rocks	1191	1
c_w	Specific heat, water	4421	2
c_{wo}	Specific heat, wollastonite-zone rock [J/(kg·K)]	1084	1
η	Viscosity of water (Pa·s)	6.6×10^{-5}	4
ΔH	Enthalpy of tremolite-consuming reaction (J/ξ)	285752	3
κ	Thermal diffusivity (m^2/s)	7.72×10^{-7}	4
k_{wo}	Permeability, wollastonite zone (m^2)	2×10^{-12}	5
k	Permeability (m^2)	1×10^{-16}	5
K_j	Thermal conductivity [W/(m·K)]	2.51	4
K_{qwo}	Hydraulic conductivity, wollastonite-zone rock [kg/(m·Pa·s)]	2.03×10^{-5}	1
K_q	Hydraulic conductivity, diopside-zone and unmetamorphosed rocks [kg/(m·Pa·s)]	1.01×10^{-9}	1
L_{di}	Heat of reaction at diopside isograd (J/kg)	57888	1
L_{wo}	Heat of reaction at wollastonite isograd (J/kg)	227227	1
p_0	Initial pressure above ambient in the stock (MPa)	100	4
ϕ	Porosity outside the wollastonite zone	0.01	1
ϕ_{wo}	Porosity inside the wollastonite zone	0.25	1
r_{di}	Location of the diopside isograd (m)		
r_{wo}	Location of the wollastonite isograd (m)		
ρ	Density, diopside-zone and unmetamorphosed rocks (kg/m^3)	2730	1
ρ_w	Density, water (kg/m^3)	666.67	2
ρ_{wo}	Density, wollastonite-zone rock (kg/m^3)	2960	1
T_0	Initial temperature above ambient of the stock (°C)	963	6
t	Time (s)		
ξ	Extent of reaction (kg^{-1})		
ω_{wo}	Hydraulic diffusivity, wollastonite zone (m^2/s)	836.6	1
ω	Hydraulic diffusivity, diopside-zone and unmetamorphosed rocks (m^2/s)	1.04	1

Initial conditions: $T = T_0$ and $p = p_0$ for $r < A$. $T = 0$ and $p = 0$ for $r > A$.

Boundary conditions: $T = 0$ and $p = 0$ for $r = \infty$.

$$K_j\left[\left(\frac{\partial T}{\partial t}\right)^+ - \left(\frac{\partial T}{\partial t}\right)^-\right] = L_{di}\rho\frac{dr_{di}}{dt} \qquad r = r_{di}$$

$$K_j\left[\left(\frac{\partial T}{\partial t}\right)^+ - \left(\frac{\partial T}{\partial t}\right)^-\right] = L_{wo}\rho\frac{dr_{wo}}{dt} \qquad r = r_{wo}$$

Heat flow:

$$[\phi\rho_w c_w + (1-\phi)\rho c]\frac{\partial T}{\partial t} = K_j\left[\frac{\partial^2 T}{\partial r^2} + \frac{2}{r}\left(\frac{\partial T}{\partial r}\right)\right] + c_w K_q\left\{\left(\frac{\partial T}{\partial r}\right)\left(\frac{\partial p}{\partial r}\right) + T\left[\frac{\partial^2 p}{\partial r^2} + \frac{2}{r}\left(\frac{\partial p}{\partial r}\right)\right]\right\} \qquad r < A,\ r > r_{di}$$

$$\left[\Delta H\frac{d\xi}{dt} + \phi\rho_w c_w + (1-\phi)\rho c\right]\frac{\partial T}{\partial t} = K_j\left[\frac{\partial^2 T}{\partial r^2} + \frac{2}{r}\left(\frac{\partial T}{\partial r}\right)\right] + c_w K_q\left\{\left(\frac{\partial T}{\partial r}\right)\left(\frac{\partial p}{\partial r}\right) + T\left[\frac{\partial^2 p}{\partial r^2} + \frac{2}{r}\left(\frac{\partial p}{\partial r}\right)\right]\right\} \qquad r_{wo} < r < r_{di}$$

$$[\phi_{wo}\rho_w c_w + (1-\phi_{wo})\rho_{wo}c_{wo}]\frac{\partial T}{\partial t} = K_j\left[\frac{\partial^2 T}{\partial r^2} + \frac{2}{r}\left(\frac{\partial T}{\partial r}\right)\right] + c_w K_{qwo}\left\{\left(\frac{\partial T}{\partial r}\right)\left(\frac{\partial p}{\partial r}\right) + T\left[\frac{\partial^2 p}{\partial r^2} + \frac{2}{r}\left(\frac{\partial p}{\partial r}\right)\right]\right\} \qquad A < r < r_{wo}$$

Fluid flow:

$$\rho_w\left(\frac{\partial \phi}{\partial t}\right) + \phi\rho_w\beta\left(\frac{\partial p}{\partial t}\right) - \phi\rho\alpha\left(\frac{\partial T}{\partial t}\right) = K_q\left[\frac{\partial^2 p}{\partial r^2} + \frac{2}{r}\left(\frac{\partial p}{\partial r}\right)\right] \qquad r < A,\ r > r_{wo}$$

$$\rho_w\left(\frac{\partial \phi}{\partial t}\right) + \phi_{wo}\rho_w\beta\left(\frac{\partial p}{\partial t}\right) - \phi_{wo}\rho_{wo}\alpha\left(\frac{\partial T}{\partial t}\right) = K_{qwo}\left[\frac{\partial^2 p}{\partial r^2} + \frac{2}{r}\left(\frac{\partial p}{\partial r}\right)\right] \qquad A < r < r_{wo}$$

* Sources: (1) This work. (2) Calculated from data of Burnham et al. (1969). (3) Calculated from data of Helgeson et al. (1978) and Burnham et al. (1969). (4) Extrapolated from data in Clark (1966), p. 300. (5) Estimated from values given by De Wiest (1965). (6) From Nabelek et al. (1986), who determined the crystallization temperature of 780 °C of the stock. To compensate for the heat of crystallization, 333 °C were added. The ambient temperature is taken to have been 150 °C.

determined for the conditions of steady fluid flux—that is, when ∇p is constant—by McKenzie (1984) and by Bickle and McKenzie (1987) and for the conditions when advection of heat is minor in comparison with conduction—that is, when the nonlinear term in Equation 15 can be neglected—by Delaney (1982). In most cases, especially those concerning the thermogravitational flow of fluid or those with complex boundary conditions, the set of equations must be solved numerically (e.g., Cathles, 1981; and Norton and Knight, 1977).

In the case of the metamorphism of the Big Horse Limestone Member, there is no evidence for substantial thermogravitational flow of fluid. The existence of horizontally stratified, relatively impervious marbles probably impeded vertically convecting fluid. The depth of the intrusion, about 6 km, lies within the realm of single-pass

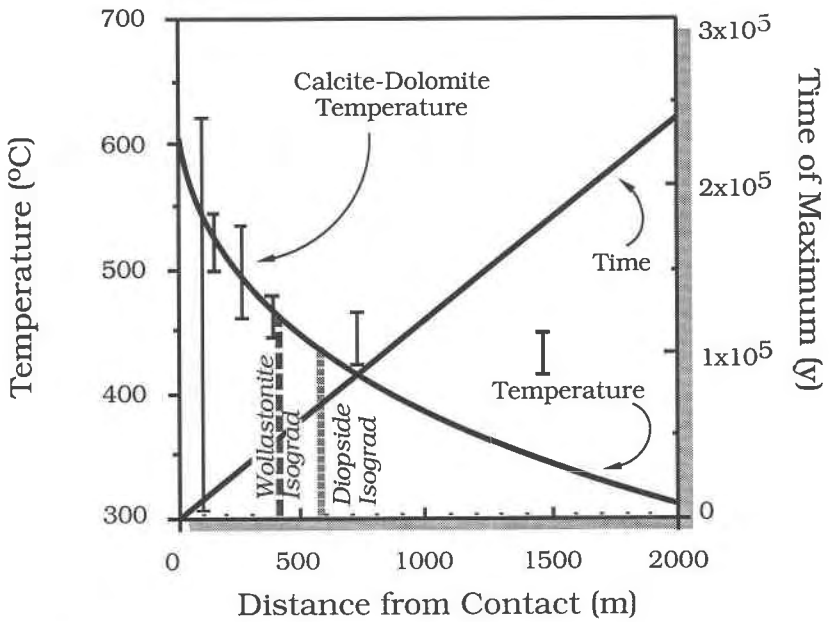

Fig. 6. Distribution of the maximum temperature in the aureole, calculated from a simple conductive heat-flow model. Calcite-dolomite temperatures are plotted according to the map distance from the contact. The true distances are probably not as great, indicating good agreement between the heat-flow model and the actual temperature. The distances of the wollastonite and diopside isograds are determined by the temperatures of 464 °C and 434 °C, respectively. The positive-sloping curve indicates the time after intrusion when the maximum was reached. The wollastonite isograd ceased advancing at ~50000 yr, and the diopside isograd stopped at ~70000 yr.

fluid flow suggested by Wood and Walther (1986). Thermogravitational convection, no doubt, played a major role in heat transport after magmatic fluids were expelled from the stock, but during metamorphism of the rocks on the margins of the stock, the significant interaction between fluid and rock occurred in the absence of gravitational recirculation.

Calculation of the heat and fluid transport through the Big Horse Limestone Member requires knowledge of several parameters: the size and geometry of the Notch Peak stock, the initial temperatures of the magma and the country rock, the fluid pressure in the stock, the physical properties of the fluid phase, and the diffusivities, permeabilities, and porosities of the rock types. Most of these simply are not known. Those that are reasonably well known are the temperature of the magma (Nabelek et al., 1986) and the intergranular porosity of the Big Horse Limestone Member, based on the present work. The thermal diffusivities of all rock types are presumed to be the same. The fluid is considered to be pure H_2O, and its thermal expansion and bulk modulus are calculated from values of specific volume given in Burnham et al. (1969). The viscosity of water was determined by extrapolation from values given by Clark (1966). Bulk porosity, i.e., intergranular porosity plus fracture porosity, and permeability are the most difficult to estimate. Two sets of values are used. The first corresponds to those of the wollastonite zone with a porosity of 0.25 and a permeability of 2 darcies, and the second to all other rocks with a porosity of 0.01 and a permeability of 10^{-4} darcies. The permeabilities were taken from those of sandstone and siltstone having similar porosities listed by De Wiest (1965). The large porosity in the wollastonite zone was surely eliminated by deformation, but as a limiting case, the porosity is assumed to have been 25%. As described below, the only effect of the large porosity is to make the porosity outside the wollastonite zone the limiting factor for the fluid flux. The porosity of 0.01 is used as a lower limit for the unmetamorphosed rocks, which have essentially no intergranular porosity, and for the stock (Norton and Knapp, 1977). All the values used in the calculations are given in Table 6. The stock is assumed to be a sphere with a radius of 8 km, intrusion is assumed to have occurred over a very short time, and the fluid flow is assumed to be radial. The fluid pressure in the stock is completely unknown. A value of 100 MPa, representing the estimated bursting strength of the granitic rock based on values reported by Clark (1966), is used in the calculations. If fluid pressures exceeded the strength, the flow of fluid through the fractured rock would very quickly have relieved this overpressure. Even in the absence of fracture development, the high fluid pressure would have been quickly dissipated by flow through rocks having the modest porosity and permeability used in these calculations, as described below.

The boundary conditions imposed by the metamorphic zones are related to the heats of reaction. At the diopside isograd, 57888 J/kg are consumed by the formation of

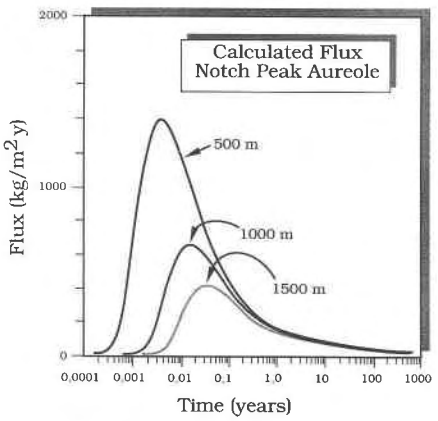

Fig. 7. Flux of water through the aureole at three distances from the contact. Even though the peak flux occurs within the first year, the major contribution to the integrated flux occurs at long times because the flux goes to zero very slowly.

the assemblage calcite + quartz + tremolite + diopside + K-feldspar + plagioclase. Thus, the difference in heat flux through this isograd is $L\rho(dx_{di}/dt)$ (Carslaw and Jaeger, 1959). Within the diopside zone, heat is continuously absorbed by the reaction tremolite + 3 calcite + 2 quartz = 5 diopside + $3CO_2$ + H_2O. The heat flow through the diopside zone is thus $[\Delta H_r(d\xi/dT) + \rho c]\,(\partial T/\partial t)$ (Labotka et al., 1984). At the wollastonite isograd, heat is absorbed at a rate of $L_{wo}\rho(dx_{wo}/dt)$, where L_{wo} is 227 000 J/kg. The porosity and permeability also differ within the wollastonite zone and outside of it. The complete set of field equations is given in Table 6.

Clearly, an analytic solution to the equations in Table 6 does not exist. The equations must be integrated numerically. A thorough development of the numerical solution of the equations is not attempted here. Rather, limits on the fluid flux can be determined from two cases: the first using the parameters for the wollastonite zone and the second using those for rocks outside the wollastonite zone. The heats of reaction are neglected. The largest of these is that of the wollastonite isograd and is only half the heat liberated by the crystallization of the magma in the stock. The boundary conditions are simply that the pressure and temperature go to zero at great distances from the contact. The initial conditions remain as listed in Table 6.

The relative contributions of conduction and advection to the heat flow are seen from the coefficients κ and $c_wK_q/(\rho c)_b$, in which $(\rho c)_b$ refers to the bulk rock plus pore water. For the conditions of the wollastonite zone, the ratio of the coefficients is 27, and, for the conditions outside the wollastonite zone, the ratio is 5.4×10^5. Thus, advection makes a small to infinitesimal contribution to the heat flow. For the purposes here, advection can be neglected. In addition, the porosity is assumed to be constant in time. Certainly, the large porosity in the wollastonite zone is eliminated by deformation, but as a limiting case, the porosity is assumed to have been constant over the time scale of the diffusion of pressure through the fluid. In the case of the wollastonite-zone conditions, this time scale is seconds, and the assumption is not unrealistic.

Within these limitations, the equations for heat and fluid flow are now described. The initial conditions are $T = T_0$, $p = p_0$, $r < A$; $T = 0$, $p = 0$, $r > A$. The boundary conditions are $T = 0$, $p = 0$, $r = \infty$. Heat flow is

$$[\phi\rho_w c_w + (1 - \phi)\rho c]\frac{\partial T}{\partial t} = K_j\left[\frac{\partial^2 T}{\partial r^2} + \frac{2}{r}\left(\frac{\partial T}{\partial r}\right)\right], \quad (17)$$

and fluid flow is

$$\phi\rho_w\beta\left(\frac{\partial p}{\partial t}\right) - \phi\rho_w\alpha\left(\frac{\partial T}{\partial t}\right) = K_q\left[\frac{\partial^2 p}{\partial r^2} + \frac{2}{r}\left(\frac{\partial p}{\partial r}\right)\right]. \quad (18)$$

These equations have the solution

$$T = \tfrac{1}{2}T_0\left[\operatorname{erf}\left(\frac{A - r}{2\sqrt{\kappa t}}\right) + \operatorname{erf}\left(\frac{A + r}{2\sqrt{\kappa t}}\right)\right] - \frac{T_0}{r}\sqrt{\frac{\kappa t}{\pi}} \cdot\left[\exp\left(\frac{-(A - r)^2}{4\kappa t}\right) - \exp\left(\frac{-(A + r)^2}{4\kappa t}\right)\right] \quad (19)$$

(Crank, 1975).

$$p = \tfrac{1}{2}T_0\frac{\alpha}{\beta}\frac{\kappa}{\kappa - \omega}\left[\operatorname{erf}\left(\frac{A - r}{2\sqrt{\kappa t}}\right) + \operatorname{erf}\left(\frac{A + r}{2\sqrt{\kappa t}}\right)\right] - \frac{T_0}{r}\frac{\alpha}{\beta}\frac{\kappa}{\kappa - \omega}\sqrt{\frac{\kappa t}{\pi}} \cdot\left[\exp\left(\frac{-(A - r)^2}{4\kappa t}\right) - \exp\left(\frac{-(A + r)^2}{4\kappa t}\right)\right] + \tfrac{1}{2}\left(p_0 - T_0\frac{\alpha}{\beta}\frac{\kappa}{\kappa - \omega}\right) \cdot\left[\operatorname{erf}\left(\frac{A - r}{2\sqrt{\omega t}}\right) + \operatorname{erf}\left(\frac{A + r}{2\sqrt{\omega t}}\right)\right] - \frac{1}{r}\left(p_0 - T_0\frac{\alpha}{\beta}\frac{\kappa}{\kappa - \omega}\right)\sqrt{\frac{\omega t}{\pi}} \cdot\left[\exp\left(\frac{-(A - r)^2}{4\omega t}\right) - \exp\left(\frac{-(A + r)^2}{4\omega t}\right)\right]. \quad (20)$$

The constants are defined in Table 6.

The maximum temperature distribution in the Notch Peak aureole, calculated from Equation 19 at the time when $\partial T/\partial t = 0$, is shown in Figure 6; the calcite + dolomite temperatures from Table 1 are also shown. There is good agreement between calculated and observed temperatures for samples within about 500 m from the contact, but the two samples at a greater distance were apparently 20 to 50 °C hotter than the calculated temperatures. This apparent discrepancy is the result of the difference between the map distance from the contact and the true distance. The error between the map and

true distance increases at great distances from the contact. The calculated temperature distribution gives the distance of the wollastonite isograd as 410 m and that of the diopside isograd as 595 m. The wollastonite-isograd position is consistent with the field evidence, but the apparent width of the diopside zone is about 1000 m, much greater than the calculated 185 m. A dip of 25° on the stock contact indicates that the true radial distance of the diopside isograd is 634 m, in close agreement with the calculated distance.

The period during prograde metamorphism was less than about 70000 yr. At that time, the diopside isograd had advanced to its greatest distance from the contact (Fig. 6). The wollastonite isograd had ceased to advance at 50000 yr after intrusion.

The fluid flux, given by $-K_q(\partial p/\partial r)$, depends on the fluid pressure within the stock, the permeability, and porosity. The fluxes at three locations, 500, 1000, and 1500 m from the contact, are shown in Figure 7 for a permeability of 10^{-16} m^2, a porosity of 1%, and an initial fluid pressure within the stock of 100 MPa. The most impressive feature of Figure 7 is that even though the maximum flux was substantial, about 1500 kg/(m^2·yr) at 500 m, pressure dissipated extremely rapidly. The pressure pulse was nearly completely dissipated within the first year after intrusion.

The value of the calculated flux depends on the choice of the initial fluid pressure. The effects of this choice on the calculated flux at a distance of 500 m are illustrated in Figure 8 for initial pressures of 50, 100, and 200 MPa. The shapes of the curves are similar, with only a slight shift in the time of peak flux. The time scale for pressure relaxation is about 0.1 yr in all cases, and the magnitude of the flux is approximately proportional to the initial pressure. For the case in which the permeability and porosity are appropriate for the wollastonite zone, the pressure completely dissipates in seconds, and, therefore, the fluid flux through the wollastonite zone was no different from that through the diopside zone.

Even though the major flux occurred almost immediately after intrusion, long before the temperature rose sufficiently for metamorphism to have occurred, the low flux that persisted for long times made the major contribution to the time-integrated water/rock ratio. The tails on the fluid-flux curves in Figures 8 and 9 approach zero only at very long times, much longer than the time period of metamorphism of $\leq 10^5$ yr. The total water/rock ratio, attributable to fluid infiltration, was calculated for the diopside- and wollastonite-zone rocks for the conditions of Figure 7. The total flux through the 434 and 464 °C isotherms, representing the diopside and wollastonite isograds, is given by

$$\mathbf{Q}_{\text{total}} = -K_q \int_0^{t_{\max}} \left(\frac{\partial p(\mathbf{r}, t)}{\partial \mathbf{r}} \right)_{T=T_{\text{isograd}}} dt. \qquad (21)$$

The value of $t_{\max}$ is 50000 yr for the wollastonite isograd

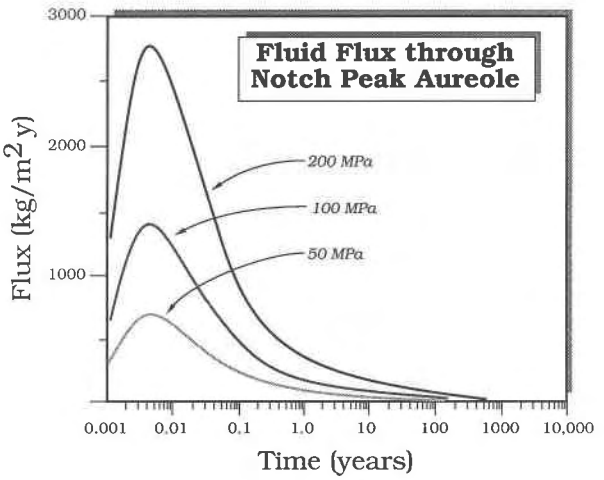

Fig. 8. Flux at 500 m for initial fluid pressures of 50, 100, and 200 MPa in the stock. The flux is approximately proportional to the pressure.

and 70000 yr for the diopside isograd. The integral in Equation 21 was evaluated numerically for the two isograds, and the results are shown in Figure 9. The positions of the two isograds and the instantaneous fluxes through the isograds over the time of metamorphism are shown in Figure 9. The flux through the isotherms is nearly independent of position because the isograds are never farther apart than 200 m and the compressibility and thermal expansion of water make small contributions to the pressure. The total flux is shown as the water/rock ratio, which is given by $\mathbf{Q}_{\text{total}}/\rho_{\text{rock}}\mathbf{r}_{\text{isograd}}$. The water/rock ratios given in Figure 9, which reach the maximum values of 0.12 for the wollastonite isograd at 50000 yr and 0.11 for the diopside isograd at 70000 yr, can be compared with those calculated from mineral equilibria if it is assumed that all the fluid that passed through the isograd equilibrated with the rock; otherwise, the values in Figure 9 must be regarded as maximum values.

Discussion

The model results depend on several simplifications and assumptions. First, the stock is assumed to have spherical geometry with a radius of 8 km. The geometry is based on the surface exposure, but the shape may not be spherical. The effect of a smaller radius on the model is to reduce the calculated width of the aureole and the amount of evolved H_2O. The simple geometry, however, results in a calculated aureole width and temperature field consistent with observations. Second, the water evolved from the crystallizing stock is assumed to present an internal pressure of 100 MPa instantaneously with emplacement. The pressure is an assumed value, and the initial condition is a simplification. Volatiles were probably released over the period of crystallization, which must have been comparable to that of metamorphism. In this case, higher fluid pressures could have been sustained for

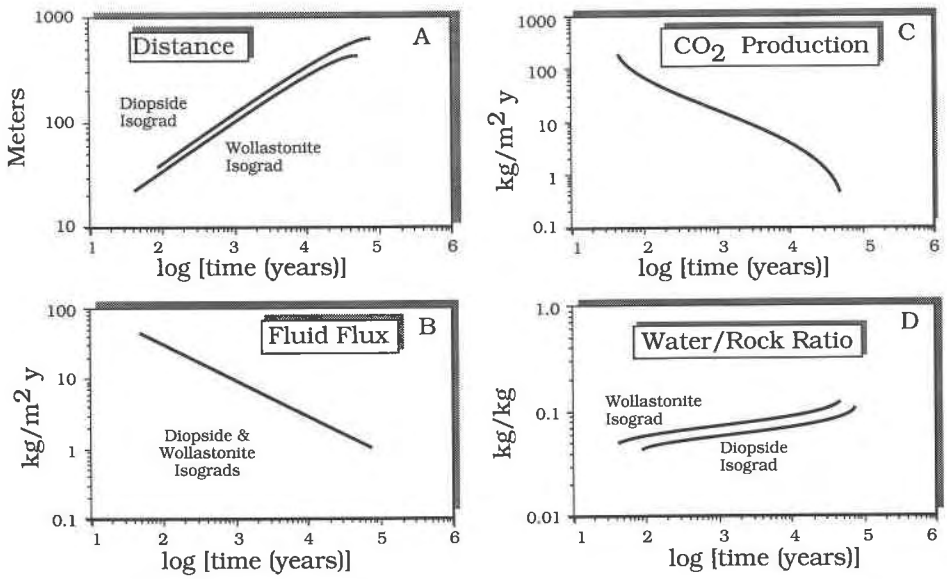

Fig. 9. Fluid flux through the diopside and wollastonite isograds. **(A)** Position of the isograds with time. At the maximum distances, the temperature reached a maximum, the rocks began to cool, and the isograds ceased to advance. **(B)** The flux through the isograds at any time after intrusion was nearly constant because of the small distance separating the isograds (cf. Fig. 7). **(C)** The rate of CO_2 produced at the wollastonite isograd was sufficiently great early in the process that the system probably was rock-dominated in the initial stages of metamorphism. **(D)** The integrated fluid flux was similar for both isograds and reached the maximum value at the temperature maximum when the reactions ceased to advance. The water/rock mass ratio was of the order of 0.1, similar to that of the diopside zone, but at least two orders of magnitude lower than that of the wollastonite zone.

longer periods, resulting in higher integrated fluxes. The magnitude of this effect can be estimated by considering that crystallization of the stock occurred on the time scale of 50000 yr and that the crystallization of the stock proceeded with $\sqrt{t}$. If the porosity was 1%, the rate of growth of pore space was 8.9×10^7 m^3/yr$^{1/2}$. If H_2O was evolved over the same time scale, a fluid pressure of 2.8 MPa could have been sustained for the period of metamorphism within the growing pore space, assuming a total amount of water of 10^{14} kg in the magma. In the steady-state limit, which gives the greatest integrated flux, if the pressure was dissipated over a distance of 10 km or greater, the water/rock ratio for metamorphic rocks would have been 0.3, or less. This value is similar to that presented in the model and to that for the diopside zone, but is only 3% or less of the apparent flux through the wollastonite zone. Thus, the difference between the observed diopside-zone flux, 0.59, and the model value, 0.11, can be accounted for in the simplified initial and boundary conditions of the model. The observed high water/rock ratio in the wollastonite zone, however, cannot be explained by inaccuracies in the model.

The water/rock ratio in Figure 9 is much too low for the value indicated by mineral equilibria in wollastonite-zone rocks (13.3). Even allowing for a 25% error in the value of x_{CO_2} because of the choice of fugacity coefficients, the water/rock ratio had to be at least 10.7 in the wollastonite zone. The wollastonite-zone rocks interacted with a far-greater quantity of H_2O than actually infiltrated the zone. The process that occurred at the infiltration front was the mixing of CO_2 generated by reaction with the reservoir of H_2O. The mixing, or diffusion, of CO_2 through the H_2O-rich fluid must have occurred at a greater rate than the diffusion of heat in order for the wollastonite isograd to have advanced isothermally. This relation is required by the change from a rock-dominated metamorphic system in the diopside zone to a fluid-dominated wollastonite zone. The rate at which CO_2 was released at the wollastonite isograd is given by $m_{CO_2}\rho_{rock}(dr_{wo}/dt)$, in which m_{CO_2} is the mass of CO_2 released (131 g per kilogram of protolith) and the derivative is the rate of advancement of the wollastonite isograd. The rate of advance of the wollastonite isograd depends on the time and distance, as can be seen in Figure 9. At small distances and times, the rate is very high, and the rate approaches 0 at 50000 yr. The rate dropped to less than 0.1 m/yr at 100 yr after intrusion, and the rate of CO_2 production was less than 36 kg/(m^2·yr) throughout most of the period of metamorphism. After 10000 yr, the rate dropped to less than 3 kg/(m^2·yr). The rate of diffusion of CO_2 through the fluid must have been fast enough to eliminate the concentration gradient between the site of generation of CO_2 and the H_2O-rich reservoir. A rough estimate of the diffusion coefficient is given by η/ρ, which is the self-diffusion coefficient in a dilute gas (Reif, 1965). For water under the conditions given in Table 6, the coefficient has a value of 2.97 m^2/yr. If CO_2 behaves similarly, the root-mean-square displacement $\sqrt{\langle r^2 \rangle}$ over the

time scale of 50000 yr, the time of formation of the wollastonite zone, is 545 m. This distance is only slightly greater than the width of the wollastonite zone, indicating that, unless turbulence aided the mixing, the characteristic times for diffusion of heat and for diffusion of CO_2 through the fluid were similar. The actual T-x_{CO_2}-t path at the wollastonite isograd was probably much more complicated than the simple steady value adopted for the calculations. Initial rapid diffusion of heat at the contact caused the generation of CO_2 by the wollastonite-isograd reactions, which buffered the fluid composition and retarded the advance of the isograd until the CO_2 mixed with the reservoir and the local value of x_{CO_2} was reduced. This close interplay probably occurred throughout the lifetime of metamorphism in the wollastonite zone and may be the cause of the complex mineral textures described by Hover-Granath et al. (1983) for these rocks.

Water/rock ratios are commonly calculated from mineral assemblages and rock compositions, either in the manner used here or by point-counting techniques. These calculated water/rock ratios rigorously indicate the amount of fluid that interacted, or equilibrated, with the rock, but do not necessarily represent the amount of fluid that flowed through the rock. There can be a great difference between the water/rock ratio and the time-integrated fluid flux. It is not easy, in most cases, to recognize the difference. The difference is quite evident at a place like Notch Peak where an isograd separates rocks with low-variance assemblages from rocks with high-variance assemblages. Here there was a change in the metamorphic system from rock-dominated to fluid-dominated. This is reflected in the water/rock ratio, which changed from ~0.6 in the rock-dominated system to ~13 in the fluid-dominated system. The large water/rock ratio indicates the size of a reservoir that interacted with the rocks. The ability of this reservoir to communicate with the rocks was greatly enhanced by the creation of substantial porosity by the decarbonation reactions that occurred at the isograd. The wollastonite isograd at Notch Peak is, then, a reaction front governed by the diffusion of heat from the stock and of CO_2 through the H_2O-rich fluid issuing from the stock.

Acknowledgments

Research on contact metamorphism by the Notch Peak stock has been funded by the Department of Energy Contract DE-AC01-82ER-12050-A001 and Grant DE-FG01-85ER-13407 to J. Papike and the National Science Foundation grants EAR 8511347 to T. Labotka and EAR 8512081 to P. Nabelek. Our thanks go to V. Hover-Granath, who first described the fascinating behavior of the Big Horse Limestone Member, and to Neal White, who ably assisted us in the field. Careful critical reviews of the manuscript by John Ferry, Simon Peacock, and Frank Spear helped us strengthen our arguments and clarify the presentation.

References cited

Bebout, G.E., and Carlson, W.D. (1986) Fluid evolution and transport during metamorphism: Evidence from the Llano uplift, Texas. Contributions to Mineralogy and Petrology, 92, 518–529.

Bickle, M.J., and McKenzie, D. (1987) The transport of heat and matter by fluids during metamorphism. Contributions to Mineralogy and Petrology, 95, 384–392.

Bird, R.B., Stewart, W.E., and Lightfoot, E.N. (1960) Transport phenomena, 780 p. Wiley, New York.

Bowers, T.S., and Helgeson, H.C. (1983a) Calculation of the thermodynamic and geochemical consequences of nonideal mixing in the system H_2O-CO_2-NaCl on phase relations in geologic systems: Equation of state for H_2O-CO_2-NaCl fluids at high pressures and temperatures. Geochimica et Cosmochimica Acta, 47, 1247–1275.

——— (1983b) Calculation of the thermodynamic and geochemical consequences of nonideal mixing in the system H_2O-CO_2-NaCl on phase relations in geologic systems: Metamorphic equilibria at high pressures and temperatures. American Mineralogist, 68, 1059–1075.

Bucher-Nurminen, K. (1981) The formation of metasomatic reaction veins in dolomitic marble roof pendants in the Bergell intrusion (Province Sondrio, northern Italy). American Journal of Science, 281, 1197–1222.

Burnham, C.W., Holloway, J.R., and Davis, N.F. (1969) Thermodynamic properties of water to 1000 °C and 10,000 bars. Geological Society of America Special Paper 132.

Carslaw, H.S., and Jaeger, J.C. (1959) Conduction of heat in solids, 510 p. Oxford University Press, New York.

Cathles, L.M. (1981) Fluid flow and genesis of hydrothermal ore deposits. Economic Geology 75th Anniversary Volume, 424–457.

Clark, S.P., Jr. (1966) Handbook of physical constants. Geological Society of America Memoir 97, 587 p.

Crank, J. (1975) The mathematics of diffusion, 414 p. Oxford University Press, New York.

Delaney, P.T. (1982) Rapid intrusion of magma into wet rock: Groundwater flow due to pore pressure increases. Journal of Geophysical Research, 87, 7739–7756.

De Wiest, R.J.M. (1965) Geohydrology, 366 p. Wiley, New York.

Ferry, J.M. (1980) A case study of the amount and distribution of heat and fluid during metamorphism. Contributions to Mineralogy and Petrology, 71, 373–385.

——— (1983) On the control of temperature, fluid composition, and reaction progress during metamorphism. American Journal of Science, 283-A, 201–232.

——— (1984) A biotite isograd in south-central Maine, U.S.A.: Mineral reactions, fluid transfer, and heat transfer. Journal of Petrology, 25, 871–893.

——— (1986) Reaction progress: A monitor of fluid-rock interaction during metamorphic and hydrothermal events. In J.V. Walther and B.J. Wood, Eds., Fluid-rock interactions during metamorphism, p. 60–88. Springer-Verlag, New York.

——— (1987) Metamorphic hydrology at 13-km depth and 400–550 °C. American Mineralogist, 72, 39–58.

Helgeson, H.C., Delany, J.M., Nesbitt, H.W., and Bird, D.K. (1978) Summary and critique of the thermodynamic properties of rock-forming minerals. American Journal of Science, 278-A, 1–299.

Hintze, L.F. (1974) Preliminary geologic map of the Notch Peak quadrangle Millard County, Utah. U.S. Geological Survey Miscellaneous Field Studies Map MF-636.

Hochella, M.F., Liou, J.G., Keskinen, M.J., and Kim, H.S. (1982) Synthesis and stability relations of magnesium idocrase. Economic Geology, 77, 798–808.

Holloway, J.R. (1977) Fugacity and activity of molecular species in supercritical fluids. In D.G. Fraser, Ed., Thermodynamics in geology, p. 161–181. Reidel, Boston.

Hover, V.C. (1981) The Notch Peak metamorphic aureole, Utah: Mineralogy, petrology, and geochemistry of the Big Horse Canyon Member of the Orr Formation. M.S. thesis, State University of New York, Stony Brook, New York.

Hover-Granath, V.C., Papike, J.J., and Labotka, T.C. (1983) The Notch Peak contact metamorphic aureole, Utah: Petrology of the Big Horse Limestone Member of the Orr Formation. Geological Society of America Bulletin, 94, 889–906.

Kerrick, D.M., and Jacobs, G.K. (1981) A modified Redlich-Kwong equation for H_2O, CO_2, and H_2O-CO_2 mixtures at elevated pressures and temperatures. American Journal of Science, 281, 735–768.

Labotka, T.C. (1981) Petrology of an andalusite-type, regional metamorphic terrain, Panamint Mountains, California. Journal of Petrology, 22, 261–296.

Labotka, T.C., and Nabelek, P.I. (1986) Petrology of the contact-metamorphosed Weeks Formation, Notch Peak, Utah. International Mineralogical Association Abstracts with Program, 147–148.

——— (1987) Isotopic exchange and the fluid/rock ratio in contact-metamorphosed calc-argillites from Notch Peak, Utah. Geological Society of American Abstracts with Programs, 19, 737.

Labotka, T.C., White, C.E., and Papike, J.J. (1984) The evolution of water in the contact-metamorphic aureole of the Duluth Complex, northeastern Minnesota. Geological Society of American Bulletin, 95, 788–804.

Labotka, T.C., Nabelek, P.I., Papike, J.J., Hover-Granath, V.C., and Laul, J.C. (1988) Effects of contact metamorphism on the chemistry of calcareous rocks in the Big Horse Limestone Member, Notch Peak, Utah. American Mineralogist, 73, 1095–1110.

McKenzie, D. (1984) The generation and compaction of partially molten rock. Journal of Petrology, 25, 713–765.

Muskat, M. (1937) The flow of homogeneous fluids through porous media, 763 p. McGraw-Hill, New York.

Nabelek, P.I., O'Neil, J.R., and Papike, J.J. (1983) Vapor phase exsolution as a controlling factor in hydrogen isotope variation in granitic rocks: The Notch Peak granitic stock, Utah. Earth and Planetary Science Letters, 66, 137–150.

Nabelek, P.I., Labotka, T.C., O'Neil, J.R., and Papike, J.J. (1984) Contrasting fluid/rock interaction between the Notch Peak granitic intrusion and argillites and limestones in western Utah: Evidence from stable isotopes and phase assemblages. Contributions to Mineralogy and Petrology, 86, 25–34.

Nabelek, P.I., Papike, J.J., and Laul, J.C. (1986) The Notch Peak granitic stock, Utah: Origin of reverse zoning and petrogenesis. Journal of Petrology, 27, 1035–1069.

Norton, D., and Knapp, R. (1977) Transport phenomena in hydrothermal systems: The nature of porosity. American Journal of Science, 277, 913–936.

Norton, D., and Knight, J. (1977) Transport phenomena in hydrothermal systems: Cooling plutons. American Journal of Science, 277, 937–981.

Papike, J.J., Cameron, K.L., and Baldwin, K. (1974) Amphiboles and pyroxenes: Characterization of other than quadrilateral components and estimates of ferric iron from microprobe data. Geological Society of America Abstracts with Programs, 6, 1053–1054.

Reif, F. (1965) Fundamentals of statistical and thermal physics, 651 p. McGraw-Hill, New York.

Rice, J.M. (1977) Progressive metamorphism of the impure dolomitic limestone in the Marysville aureole, Montana. American Journal of Science, 277, 1–24.

——— (1983) Metamorphism of rodingites: Part I. Phase relations in a portion of the system CaO-MgO-Al_2O_3-SiO_2-CO_2-H_2O. American Journal of Science, 283-A, 121–150.

Rice, J.M., and Ferry, J.M. (1982) Buffering, infiltration, and the control of intensive variables during metamorphism. Mineralogical Society of America Reviews in Mineralogy, 10, 263–326.

Rumble, D., III, Ferry, J.M., Hoering, T.C., and Boucot, A.J. (1982) Fluid flow during metamorphism at the Beaver Brook fossil locality, New Hampshire. American Journal of Science, 282, 886–919.

Shmonov, V.M., and Shmulovich, K.I. (1974) Molal volumes and equation of state of CO_2 at temperatures from 100 to 1000 °C and pressures from 2000 to 10,000 bars. Akademiya Nauk SSSR Doklady, 217, 206–209.

Thompson, J.B., Jr., Laird, J., and Thompson, A.B. (1982) Reactions in amphibolite, greenschist, and blueschist. Journal of Petrology, 23, 1–27.

Trommsdorff, V., and Skippen, G. (1986) Vapour loss ("boiling") as a mechanism for fluid evolution in metamorphic rocks. Contributions to Mineralogy and Petrology, 94, 317–322.

Valley, J.W., Peacor, D.R., Bowman, J.R., Essene, E.J., and Allard, M.J. (1985) Crystal chemistry of a Mg-vesuvianite and implications of phase equilibria in the system CaO-MgO-Al_2O_3-SiO_2-H_2O-CO_2. Journal of Metamorphic Geology, 3, 137–153.

Walther, J.V., and Orville, P.M. (1982) Volatile production and transport in regional metamorphism. Contributions to Mineralogy and Petrology, 79, 252–257.

Wood, B.J., and Walther, J.V. (1986) Fluid flow during metamorphism and its implications for fluid-rock ratios. In J.V. Walther and B.J. Wood, Eds., Fluid-rock interactions during metamorphism, p. 89–108. Springer-Verlag, New York.

Manuscript received September 14, 1987
Manuscript accepted July 29, 1988